ISSN 2667-4211

ESKİŞEHİR TECHNICAL UNIVERSITY JOURNAL OF SCIENCE AND TECHNOLOGY

A – Applied Sciences and Engineering

Volume 24 Number 3 - September - 2023

ESKİŞEHİR TECHNICAL UNIVERSITY JOURNAL OF SCIENCE AND TECHNOLOGY
A- Applied Sciences and Engineering
Eskişehir Teknik Üniversitesi Bilim ve Teknoloji Dergisi A – Uygulamalı Bilimler ve Mühendislik

Volume: 24 / Number: 3 / September - 2023

Eskişehir Technical University Journal of Science and Technology A - Applied Sciences and Engineering (ESTUJST-A) is a peer-reviewed and refereed international journal published by Eskişehir Technical University. Since 2000, it has been regularly published and distributed biannually and it has been published quarterly and only electronically since 2016.
The journal accepts only manuscripts written in English.

The journal issues are published electronically in **March, June**, **September**, and **December**.

Eskişehir Technical University Journal of Science and Technology A - Applied Sciences and Engineering is an international peer-reviewed and refereed journal published by Eskişehir Technical University.

The journal is dedicated to the dissemination of knowledge in applied sciences and engineering disciplines.

The journal aims to publish high quality, original international scientific research articles with specific contributions to the literature in the field of engineering and applied sciences. The journal publishes research papers in the fields of applied science and technology such as Physics, Biology, Mathematics, Statistics, Chemistry and Chemical Engineering, Environmental Sciences and Engineering, Civil Engineering, Earth and Atmospheric Sciences, Electrical and Electronical Engineering, Computer Science and Informatics, Materials Sciences and Engineering, Mechanical Engineering, Mining Engineering, Industrial Engineering, Aeronautics and Astronautics, Pharmaceutical Sciences.

The journal publishes original research articles and special issue articles. All articles are peer-reviewed and the articles that have been evaluated are ensured to meet with researchers as soon as possible.

"Anadolu Üniversitesi Bilim ve Teknoloji Dergisi A - Uygulamalı Bilimler ve Mühendislik (Anadolu University Journal of Science and Technology A - Applied Sciences and Engineering)" published within Anadolu University started to be published within Eskişehir Technical University which was established due to statute law 7141, in 2018. Hence, the name of the journal is changed to " Eskişehir Technical University Journal of Science and Technology A - Applied Sciences and Engineering (Eskişehir Teknik Üniversitesi Bilim ve Teknoloji Dergisi A - Uygulamalı Bilimler ve Mühendislik)".

Indexed by **ULAKBIM TR Dizin**

ESKİŞEHİR TECHNICAL UNIVERSITY JOURNAL OF SCIENCE AND TECHNOLOGY
A- Applied Sciences and Engineering
Eskişehir Teknik Üniversitesi Bilim ve Teknoloji Dergisi A – Uygulamalı Bilimler ve Mühendislik

Volume: 24 / Number: 3 / September– 2023

Owner / Publisher: Prof. Dr. Adnan ÖZCAN for Eskişehir Technical University

CONTACT INFORMATION
Eskişehir Technical Unıversity Journal of Science and Technology
Eskişehir Technical University, Institute of Graduate Programs, 26470 Eskişehir, TURKEY
Phone: +90 222 213 7485
e-mail : btda@eskisehir.edu.tr

ESKİŞEHİR TECHNICAL UNIVERSITY JOURNAL OF SCIENCE AND TECHNOLOGY
A- Applied Sciences and Engineering

Eskişehir Teknik Üniversitesi Bilim ve Teknoloji Dergisi A – Uygulamalı Bilimler ve Mühendislik

Volume: 24 / Number: 3 / September - 2023

ESKİŞEHİR TECHNICAL UNIVERSITY JOURNAL OF SCIENCE AND TECHNOLOGY
A- Applied Sciences and Engineering
Eskişehir Teknik Üniversitesi Bilim ve Teknoloji Dergisi A – Uygulamalı Bilimler ve Mühendislik

ABOUT

Eskişehir Technical University Journal of Science and Technology A - Applied Sciences and Engineering (ESTUJST-A) is a peer-reviewed and refereed international journal published by Eskişehir Technical University. Since 2000, it has been regularly published and distributed biannually and it has been published quarterly and only electronically since 2016.

The journal accepts only manuscripts written in English.

The journal issues are published electronically in **MARCH, JUNE, SEPTEMBER**, and **DECEMBER.**

AIM AND SCOPE

Eskişehir Technical University Journal of Science and Technology A - Applied Sciences and Engineering is an international peer-reviewed and refereed journal published by Eskişehir Technical University.

The journal is dedicated to the dissemination of knowledge in applied sciences and engineering disciplines.

The journal aims to publish high quality, original international scientific research articles with specific contributions to the literature in the field of engineering and applied sciences. The journal publishes research papers in the fields of applied science and technology such as Physics, Biology, Mathematics, Statistics, Chemistry and Chemical Engineering, Environmental Sciences and Engineering, Civil Engineering, Earth and Atmospheric Sciences, Electrical and Electronical Engineering, Computer Science and Informatics, Materials Sciences and Engineering, Mechanical Engineering, Mining Engineering, Industrial Engineering, Aeronautics and Astronautics, Pharmaceutical Sciences.

The journal publishes original research articles and special issue articles. All articles are peer-reviewed and the articles that have been evaluated are ensured to meet with researchers as soon as possible.

PEER REVIEW PROCESS

Manuscripts are first reviewed by the editorial board in terms of its its journal's style rules scientific content, ethics and methodological approach. If found appropriate, the manuscript is then send to at least two renown referees by editor. The decision in line with the referees may be an acceptance, a rejection or an invitation to revise and resubmit. Confidential review reports from the referees will be kept in archive. All submission process manage through the online submission systems.

OPEN ACCESS POLICY

This journal provides immediate open access to its content on the principle that making research freely available to the public supports a greater global exchange of knowledge.

PRICE POLICY

Eskişehir Technical University Journal of Science and Technology A - Journal of Applied Sciences and Engineering is an English, peer-reviewed, scientific, free of charge open-access-based journal. The author is not required to pay any publication fees or article processing charges (APCs) for peer-review administration and management, typesetting, and open-access. Articles also receive Digital Object Identifiers (DOIs) from the CrossRef organization to ensure they are always available.

ETHICAL RULES

You can reach the Ethical Rules in our journal in full detail from the link below:

https://dergipark.org.tr/en/pub/estubtda/policy

Ethical Principles and Publication Policy

Policy & Ethics

Assessment and Publication

As a peer-reviewed journal, it is our goal to advance scientific knowledge and understanding. We adhere to the guideline and ethical standards from the Committee on Publication Ethics (COPE) and the recommendations of ICMJE (International Committee of Medical Journal Editors) regarding all aspects of publication ethics and cases of research and publication misconduct to ensure that all publications represent accurate and original work and that our peer review process is structured without bias. We have outlined a set of ethical principles that must be followed by all authors, reviewers, and editors.

All manuscripts submitted to our journals are pre-evaluated in terms of their relevance to the scope of the journal, language, compliance with writing instructions, suitability for science, and originality, by taking into account the current legal requirements regarding copyright infringement and plagiarism. Manuscripts that are evaluated as insufficient or non-compliant with the instructions for authors may be rejected without peer review.

Editors and referees who are expert researchers in their fields assess scientific manuscripts submitted to our journals. A blind peer review policy is applied to the evaluation process. The Editor-in-Chief, if he/she sees necessary, may assign an Editor for the manuscript or may conduct the scientific assessment of the manuscript himself/herself. Editors may also assign referees for the scientific assessment of the manuscript and make their decisions based on reports by the referees. The Editor-in-Chief makes the final decision regarding the publishing of the manuscript.

Articles are accepted for publication by the Editor-in-Chief in accordance with the COPE (Committee on Publication Ethics). Authors can access this information online via the journals' websites (https://publicationethics.org/). Articles are accepted for publication on the understanding that they have not been published and are not going to be considered for publication elsewhere. Authors should certify that neither the manuscript nor its main contents have already been published or submitted for publication in another journal.

The journal adapts the COPE guidelines to satisfy the high-quality standards of ethics for authors, editors, and reviewers:

Duties of Editors-in-Chief and co-Editors

The crucial role of the journal Editor-in-Chief and co-Editors is to monitor and ensure the fairness, timeliness, thoroughness, and civility of the peer-review editorial process. The main responsibilities of Editors-in-Chief are as follows:

• Selecting manuscripts suitable for publication while rejecting unsuitable manuscripts,
• Ensuring a supply of high-quality manuscripts to the journal by identifying important,
• Increasing the journal's impact factor and maintaining the publishing schedule,
• Providing strategic input for the journal's development,

Duties of Editors

The main responsibilities of editors are as follows:

• An editor must evaluate the manuscript objectively for publication, judging each on its quality without considering the nationality, ethnicity, political beliefs, race, religion, gender, seniority, or institutional affiliation of the author(s). Editors should decline any assignment when there is a potential for conflict of interest.
• Editors must ensure the document(s) sent to the reviewers does not contain information of the author(s) and vice versa.
• Editors' decisions should be provided to the author(s) accompanied by the reviewers' comments and recommendations unless they contain offensive or libelous remarks.
• Editors should respect requests (if well reasoned and practicable) from author(s) that an individual should not review the submission.
• Editors and all staff members should guarantee the confidentiality of the submitted manuscript.
• Editors should have no conflict of interest with respect to articles they reject/accept. They must not have a conflict of interest with the author(s), funder(s), or reviewer(s) of the manuscript.
• Editors should strive to meet the needs of readers and authors and to constantly improve the journal.

Duties of Reviewers/Referees

The main responsibilities of reviewers/referees are as follows:

• Reviewers should keep all information regarding papers confidential and treat them as privileged information.
• Reviews should be conducted objectively, with no personal criticism of the author.
• Reviewers assist in the editorial decision process and as such should express their views clearly with supporting arguments.
• Reviewers should complete their reviews within a specified timeframe (maximum thirty-five (35) days). In the event that a reviewer feels it is not possible for him/her to complete the review of the manuscript within a stipulated time, then this information must be communicated to the editor so that the manuscript could be sent to another reviewer.
• Unpublished materials disclosed in a submitted manuscript must not be used in a reviewer's personal research without the written permission of the author. Information contained in an unpublished manuscript will remain confidential and must not be used by the reviewer for personal gain.
• Reviewers should not review manuscripts in which they have conflicts of interest resulting from competitive, collaborative, or other relationships or connections with any of the authors, companies, or institutions connected to the papers.

• Reviewers should identify similar work in published manuscripts that has not been cited by the author. Reviewers should also notify the Editors of significant similarities and/or overlaps between the manuscript and any other published or unpublished material.

Duties of Authors

The main responsibilities of authors are as follows:

• The author(s) should affirm that the material has not been previously published and that they have not transferred elsewhere any rights to the article.
• The author(s) should ensure the originality of the work and that they have properly cited others' work in accordance with the reference format.
• The author(s) should not engage in plagiarism or in self-plagiarism.
• On clinical and experimental humans and animals, which require an ethical committee decision for research in all branches of science;
All kinds of research carried out with qualitative or quantitative approaches that require data collection from the participants by using survey, interview, focus group work, observation, experiment, interview techniques,
Use of humans and animals (including material/data) for experimental or other scientific purposes,
• Clinical studies on humans,
• Studies on animals,
• Retrospective studies in accordance with the law on the protection of personal data, (Ethics committee approval should have been obtained for each individual application, and this approval should be stated and documented in the article.)
Information about the permission (board name, date, and number) should be included in the "Method" section of the article and also on the first/last page.
During manuscript upload, the "Ethics Committee Approval" file should be uploaded to the system in addition to the manuscript file.
In addition, in case reports, it is necessary to include information on the signing of the informed consent/ informed consent form in the manuscript.
• The author(s) should suggest no personal information that might make the identity of the patient recognizable in any form of description, photograph, or pedigree. When photographs of the patient were essential and indispensable as scientific information, the author(s) have received consent in written form and have clearly stated as much.
• The author(s) should provide the editor with the data and details of the work if there are suspicions of data falsification or fabrication. Fraudulent data shall not be tolerated. Any manuscript with suspected fabricated or falsified data will not be accepted. A retraction will be made for any publication which is found to have included fabricated or falsified data.
• The author(s) should clarify everything that may cause a conflict of interests such as work, research expenses, consultant expenses, and intellectual property.
• The author(s) must follow the submission guidelines of the journal.
• The author(s) discover(s) a significant error and/or inaccuracy in the submitted manuscript at any time, then the error and/or inaccuracy must be reported to the editor.
• The author(s) should disclose in their manuscript any financial or other substantive conflicts of interest that might be construed to influence the results or interpretation of their manuscript. All sources of financial support should be disclosed under the heading of "Acknowledgment" or "Contribution".
• The corresponding author should ensure that all appropriate co-authors and no inappropriate co-authors are included in the paper and that all co-authors have seen and approved the final version of the paper and have agreed to its submission for publication. All those who have made

significant contributions should be listed as co-authors. Others who have participated in certain substantive aspects of the research should be acknowledged or listed under the heading of "Author Contributions".

Cancellations/Returns

Articles/manuscripts may be returned to the authors in order to increase the authenticity and/or reliability and to prevent ethical breaches, and even if articles have been accepted and/or published, they can be withdrawn from publication if necessary. The Editor-in-Chief of the journal has the right to return or withdraw an article/manuscript in the following situations:

• When the manuscript is not within the scope of the journal,
• When the scientific quality and/or content of the manuscript do not meet the standards of the journal and a referee review is not necessary,
• When there is proof of ruling out the findings obtained by the research, (When the article/manuscript is undergoing an assessment or publication process by another journal, congress, conference, etc.,)
• When the article/manuscript was not prepared in compliance with scientific publication ethics,
• When any other plagiarism is detected in the article/manuscript,
• When the authors do not perform the requested corrections within the requested time (maximum twenty-one (21) days),
• When the author does not submit the requested documents/materials/data etc. within the requested time,
• When the requested documents/materials/data etc. submitted by the author are missing for the second time,
• When the study includes outdated data,
• When the authors make changes that are not approved by the editor after the manuscript was submitted,
• When an author is added/removed, the order of the authors is changed, the corresponding author is changed, or the addresses of the authors are changed without the consent of the Editor-in-Chief,
• When a statement is not submitted indicating that approval of the ethics committee permission was obtained for the following (including retrospective studies):
• When human rights or animal rights are violated,

ETHICAL ISSUES

Plagiarism

The use of someone else's ideas or words without a proper citation is considered plagiarism and will not be tolerated. Even if a citation is given, if quotation marks are not placed around words taken directly from other authors' work, the author is still guilty of plagiarism. Reuse of the author's own previously published words, with or without a citation, is regarded as self-plagiarism.

All manuscripts received are submitted to iThenticate®, which compares the content of the manuscript with a database of web pages and academic publications. Manuscripts are judged to be plagiarized or self-plagiarized, based on the iThenticate® report or any other source of information, will be rejected. Corrective actions are proposed when plagiarism and/or self-plagiarism is detected after publication. Editors should analyze the article and decide whether a corrected article or retraction needs to be published.

Open-access theses are considered as published works and they are included in the similarity checks.

iThenticate® report should have a maximum of 11% from a single source, and a maximum of 25% in total.

Conflicts of Interest

Eskişehir Technical University Journal of Science and Technology A - Applied Sciences and Engineering should be informed of any significant conflict of interest of editors, authors, or reviewers to determine whether any action would be appropriate (e.g. an author's statement of conflict of interest for a published work, or disqualifying a referee).

Financial

The authors and reviewers of the article should inform the journal about the financial information that will bring financial gain or loss to any organization from the publication of the article.

*Research funds; funds, consulting fees for a staff member; If you have an interest, such as patent interests, you may have a conflict of interest that needs to be declared.

Other areas of interest

The editor or reviewer may disclose a conflict of interest that, if known, would be embarrassing (for example, an academic affiliation or rivalry,a close relationship or dislike, or a person who may be affected by the publication of the article).

Conflict of interest statement

Please note that a conflict of interest statement is required for all submitted manuscripts. If there is no conflict of interest, please state "There are no conflicts of interest to declare" in your manuscript under the heading "Conflicts of Interest" as the last section before your Acknowledgments.

AUTHOR GUIDELINES

All manuscripts must be submitted electronically.

You will be guided stepwise through the creation and uploading of the various files. There are no page charges. Papers are accepted for publication on the understanding that they have not been published and are not going to be considered for publication elsewhere. Authors should certify that neither the manuscript nor its main contents have already been published or submitted for publication in another journal. We ask a signed copyright to start the evaluation process. After a manuscript has been submitted, it is not possible for authors to be added or removed or for the order of authors to be changed. If authors do so, their submission will be cancelled.

Manuscripts may be rejected without peer review by the editor-in-chief if they do not comply with the instructions to authors or if they are beyond the scope of the journal. After a manuscript has been accepted for publication, i.e. after referee-recommended revisions are complete, the author will not be permitted to make any changes that constitute departures from the manuscript that was accepted by the editor. Before publication, the galley proofs are always sent to the authors for corrections. Mistakes or omissions that occur due to some negligence on our part during final printing will be rectified in an errata section in a later issue.

This does not include those errors left uncorrected by the author in the galley proof. The use of someone else's ideas or words in their original form or slightly changed without a proper citation is considered plagiarism and will not be tolerated. Even if a citation is given, if quotation marks are not placed around words taken directly from another author's work, the author is still guilty of plagiarism. All manuscripts received are submitted to iThenticateR, a plagiarism checking system, which compares the content of the manuscript with a vast database of web pages and academic publications. In the received iThenticateR report; The similarity rate is expected to be below 25%. Articles higher than this rate will be rejected.

Uploading Articles to the Journal
Authors should prepare and upload 2 separate files while uploading articles to the journal. First, the Author names and institution information should be uploaded so that they can be seen, and then (using the additional file options) a separate file should be uploaded with the Author names and institution information completely closed. When uploading their files with closed author names, they will select the "Show to Referee" option, so that the file whose names are closed can be opened to the referees.

Prepatation of Manuscript

Style and Format
Manuscripts should be **single column** by giving one-spaced with 2.5-cm margins on all sides of the page, in Times New Roman font (font size 11). Every page of the manuscript, including the title page, references, tables, etc., should be numbered. All copies of the manuscript should also have line numbers starting with 1 on each consecutive page.

Manuscripts must be upload as word document (*.doc, *.docx vb.). **Please avoid uploading *texts in *.pdf format.***

Symbols, Units and Abbreviations
Standard abbreviations and units should be used; SI units are recommended. Abbreviations should be defined at first appearance, and their use in the title and abstract should be avoided. Generic names of chemicals should be used. Genus and species names should be typed in italic or, if this is not available, underlined.

Please refer to equations with capitalisation and unabbreviated (e.g., as given in Equation (1)).

Manuscript Content
Articles should be divided into logically ordered and numbered sections. Principal sections should be numbered consecutively with Arabic numerals (1. Introduction, 2. Formulation of problem, etc.) and subsections should be numbered 1.1., 1.2., etc. Do not number the Acknowledgements or References sections. The text of articles should be, if possible, divided into the following sections: Introduction, Materials and Methods (or Experimental), Results, Discussion, and Conclusion.

Title and contact information
The first page should contain the full title in sentence case (e.g., Hybrid feature selection for text classification), the full names (last names fully capitalised) and affiliations (in English) of all authors (Department, Faculty, University, City, Country, E-mail), and the contact e-mail address for the clearly identified corresponding author. The first page should contain the full title, abstract and keywords (both English and Turkish).

Abstract
The abstract should provide clear information about the research and the results obtained, and should not exceed 300 words. The abstract should not contain citations and must be written in Times New Roman font with font size 9.

Keywords
Please provide 3 to 5 keywords which can be used for indexing purposes.

Introduction
The motivation or purpose of your research should appear in the "Introduction", where you state the questions you sought to answer, and then provide some of the historical basis for those questions.

Methods
Provide sufficient information to allow someone to repeat your work. A clear description of your experimental design, sampling procedures, and statistical procedures is especially important in papers describing field studies, simulations, or experiments. If you list a product (e.g., animal food, analytical device), supply the name and location of the manufacturer. Give the model number for equipment used.

Results
Results should be stated concisely and without interpretation.

Discussion
Focus on the rigorously supported aspects of your study. Carefully differentiate the results of your study from data obtained from other sources. Interpret your results, relate them to the results of previous research, and discuss the implications of your results or interpretations.

Conclusion
This should state clearly the main conclusions of the research and give a clear explanation of their importance and relevance. Summary illustrations may be included.

Acknowledgments
Acknowledgments of people, grants, funds, etc. should be placed in a separate section before the reference list. The names of funding organizations should be written in full.

Conflict of Interest Statement

The authors are obliged to present the conflict of interest statement at the end of the article after the acknowledgments section.

Author Contributions
All authors, author contributions and contribution rates should be clearly stated.

References
Writting Style; **AMA; References Writting format** should be used in the reference writing of our journal. If necessary, at this point, the reference writings of the articles published in our article can be examined.

Citations in the text should be identified by numbers in square brackets. The list of references at the end of the paper should be given in order of their first appearance in the text. All authors should be included in reference lists unless there are 10 or more, in which case only the first 10 should be given, followed by 'et al.'. Do not use individual sets of square brackets for citation numbers that appear together, e.g., [2,3,5–9], not [2], [3], [5]–[9]. Do not include personal communications, unpublished data, websites, or other unpublished materials as references, although such material may be inserted (in parentheses) in the text. In the case of publications in languages other than English, the published English title should be provided if one exists, with an annotation such as "(article in Turkish with an abstract in English)". If the publication was not

published with an English title, cite the original title only; do not provide a self-translation. References should be formatted as follows (please note the punctuation and capitalisation):

Journal articles
Journal titles should be abbreviated according to ISI Web of Science abbreviations.
Guyon I, Elisseeff A. An introduction to variable and feature selection. J Mach Learn Res 2003; 3: 1157-1182.

Izadpanahi S, Ozcınar C, Anbarjafari G, Demirel H. Resolution enhancement of video sequences by using discrete wavelet transform and illumination compensation. Turk J Elec Eng & Comp Sci 2012; 20: 1268-1276.

Books
Haupt RL, Haupt SE. Practical Genetic Algorithms. 2nd ed. New York, NY, USA: Wiley, 2004.
Kennedy J, Eberhart R. Swarm Intelligence. San Diego, CA, USA: Academic Press, 2001.

Chapters in books
Poore JH, Lin L, Eschbach R, Bauer T. Automated statistical testing for embedded systems. In: Zander J, Schieferdecker I, Mosterman PJ, editors. Model-Based Testing for Embedded Systems. Boca Raton, FL, USA: CRC Press, 2012. pp. 111-146.

Conference proceedings
Li RTH, Chung SH. Digital boundary controller for single-phase grid-connected CSI. In: IEEE 2008 Power Electronics Specialists Conference; 15–19 June 2008; Rhodes, Greece. New York, NY, USA: IEEE. pp. 4562-4568.

Theses
Boynukalın Z. Emotion analysis of Turkish texts by using machine learning methods. MSc, Middle East Technical University, Ankara, Turkey, 2012.

Tables and Figures
All illustrations (photographs, drawings, graphs, etc.), not including tables, must be labelled "Figure." Figures must be submitted in the manuscript.

All tables and figures must have a caption and/or legend and be numbered (e.g., Table 1, Figure 2), unless there is only one table or figure, in which case it should be labelled "Table" or "Figure" with no numbering. Captions must be written in sentence case (e.g., Macroscopic appearance of the samples.). The font used in the figures should be Times New Roman. If symbols such as ×, μ, η, or ν are used, they should be added using the Symbols menu of Word.

All tables and figures must be numbered consecutively as they are referred to in the text. Please refer to tables and figures with capitalisation and unabbreviated (e.g., "As shown in Figure 2…", and not "Fig. 2" or "figure 2").

The resolution of images should not be less than 118 pixels/cm when width is set to 16 cm. Images must be scanned at 1200 dpi resolution and submitted in jpeg or tiff format. Graphs and diagrams must be drawn with a line weight between 0.5 and 1 point. Graphs and diagrams with a line weight of less than 0.5 point or more than 1 point are not accepted. Scanned or photocopied graphs and diagrams are not accepted.

Figures that are charts, diagrams, or drawings must be submitted in a modifiable format, i.e. our graphics personnel should be able to modify them. Therefore, if the program with which the figure is drawn has a “save as” option, it must be saved as *.ai or *.pdf. If the “save as” option does not include these extensions, the figure must be copied and pasted into a blank Microsoft Word document as an editable object. It must not be pasted as an image file (tiff, jpeg, or eps) unless it is a photograph.

Tables and figures, including caption, title, column heads, and footnotes, must not exceed 16 × 20 cm and should be no smaller than 8 cm in width. For all tables, please use Word’s “Create Table” feature, with no tabbed text or tables created with spaces and drawn lines. Please do not duplicate information that is already presented in the figures.

Article Corrections and Uploading to the System

Authors should upload the desired edits for their articles without destroying or changing the Template file of the article, by selecting and specifying the relevant edits as Colored, and also submit the Clean version of the article in 2 separate files (using the Additional file option if necessary). * In case of submitting a corrected article, a separate File in Reply to the Referees must be prepared and the "Reply to the Referees" option in the Add additional file option should be checked and uploaded. If a separate file is not prepared in response to the referees, the Author will definitely be asked to upload the relevant file again and the evaluation will be in the pending phase.

ESKİŞEHİR TECHNICAL UNIVERSITY JOURNAL OF SCIENCE AND TECHNOLOGY
A – Applied Sciences and Engineering
Volume: 24 / Number: 3 / September - 2023

CONTENTS

RESEARCH ARTICLE

ESKİŞEHİR TECHNICAL UNIVERSITY JOURNAL OF SCIENCE AND TECHNOLOGY
A- APPLIED SCIENCES AND ENGINEERING

2023, 24(3), pp. 164-176, DOI:10.18038/estubtda.1197024

RESEARCH ARTICLE

ENHANCEMENT OF HEAT TRANSFER WITH VISCOUS DISSIPATION IMPACT ON FLUID FLOW PAST A MOVING WEDGE IN A PERMEABLE DOMAIN

Uchenna Awucha UKA [1], Innocent Chukwuemeka EMEZIEM [2], Semiu Akinpelu AYINDE [3]

Charles ADENIKA [3], Kelvin Onyekwere AGBO [3]

[1, 3] Department of Basic Sciences, School of Science and Technology, Babcock University, Ogun State, 121003, Nigeria

[2]Department of Mathematics, College of Physical and Applied Sciences, Michael Okpara University of Agriculture, Umudike, Abia State, 440101, Nigeria

ABSTRACT

The problem of modelling and analysis of fluid flow in the presence of viscous dissipation as a result of a wedge in motion is analytically and numerically deliberated upon. The much-valued significance of this study in the aspects of technological and industrial revolution include aerospace, oil recovery systems, defence machineries, extrusion, moulding and polymerisation of sheets, building of war arsenal and glass whirling. However, the frontiers of several physical problems are modelled by both partial and ordinary differential equations (PDEs and ODEs). Therefore, the mathematical modelling of our present problem is not an exemption. Hence, the PDEs in which our problem under consideration is modelled become reformed into coupled ODEs in nonlinear form through the deployment of adequate and standard conversion procedure with dimensionless variables. In line with the approach of our solution methodology, the boundary conditions governing the flow models are also transmuted. Afterwards, the well-established regular perturbation skill aided in the resolution of the problem. The solutions realized are simulated through the adoption of a software package (Mathematica V.10 scheme) for the numerical solutions. Our numerical results are embodied in form of graphs and legends. It is worthy to note that an increase in the rate of flow remains a function of effect of rising values of the porosity and Grashof thermal parameters whereas the opposite behaviour of the flow field is linked to improving values of suction parameter. Also, the enhancement of the suction parameter and Eckert number breeds intensification in the temperature. Similarly, an enhancement in the values of Prandtl number, $Pr = 0.7,\ 1.5,\ 5.0,\ 7.0$ with radiation parameter, $A = 0.1$, and Eckert number $Ec = 0.2$ showed an increase in the rate of heat transfer i.e., $-\varphi'(0) = 0.7594,\ 1.9077,\ 10.5114,\ 17.9537$. Hence, the Nusselt number intensifies with the rising values of the Prandtl parameter.

Keywords: Heat transference, Porous medium, Perturbation, Simulation, Viscosity

1. INTRODUCTION

The study of fluid viscosity forms an important part of thermal augmentation in its application to heat exchangers machinery. The fluid viscidness helps in transferring and transforming thermal energy across the flowing fluid and this process impacts hotness to the fluid. Hence, this partly irretrievable procedure is termed viscous dissipation. Thus, the shear strain plays a vital role in the transformation, thermally. The significance of this research is valued in the area of scheming chilling devices, thermal loss of different forms in improving thermal conductivity characteristics of an isothermal flow leading to a surge in their technological advancement and applications. Meanwhile, in the study of fluid flows over a wedge, informs a typical issue in the general behavioural pattern of dynamical fluid system. Therefore, applications of wedge flow ranges from mechanical, petrochemical, geological engineering and technology etc. Hence, the progress made in controlling and enhancing the rate of thermal conductivity in various engineering, technological, production, metallurgical and packaging firms cannot be overemphasised. The initial investigation of incompressible fluid viscosity past a wedge using the Falkner-Skan equation remains the concept of [1]. The analytical simulation of this equation using

*Corresponding Author: ukau@babcock.edu.ng
Received: 31.10.2022 Published: 22.09.2023

numerical dwindling velocity distribution was studied by [2]. Lately, several researchers developed keen interest in studying transmission of fluid over a wedge material. Thus, the deployment of Dirichlet with Robin heat conditions at the boundary was studied by [3, 4, 5]. Later on, Shit and Majee [6] examined the influence of heat radiation and chemical reaction on MHD fluid passage over a dual disposed elastic plate with non-constant viscosity due to thermal source/sink. They inferred that radiation as well as heat source/sink determines to a large extent, the rate at which heat is conveyed at wall section. The numerical analysis involving hydromagnetic slip movement of liquid filled with nanofluid over a wedge in the presence of convectively thermal source/drip was shared by [7].

The application of chemical reactions in the presence of fluid flow has proved very useful in diverse industrial uses, such as in food handling firms and paint production companies, etc. Hence, Sulochana et al. [8] through analytical means studied free and forced convection Casson nanofluid past a diagonal material. They maintained that improved concentration of fluid and transmission mass ratio is achieved because of appreciating values of chemical reactivity. The MHD Falkner-Skan wall layer passage with interior energy supply/drop was discussed by [9]. Their result established a difference in heat supply/lag on transmission speed of thermal energy when compared to its rate on the skin-friction coefficient. Few years ago, some research on nanofluid flow over a wedge has been carried out by [10, 11, 12 and 13]. The report on non-Newtonian equation over a nonlinearly elongating plate with different external factors was achieved by [14]. However, Aman et al. [15] inspected a nanofluid flow with small-particles in form of gold due to the impact of radiation as well as transverse diffusion on the distribution field. A fluid prototype surrounded by Riga sheets with an architype flow having stretching and viscosity features amid a sloping conduit has been established by [16, 17]. In recent times, Ullah et al. [18] explored the inspiration of enforced Lorentz effects on a non-Newtonian flow. Similarly, flow over a wall layered nanofluid past a moving wedge was presented by [19]. An examination on the flow and thermal transportation characteristics in a viscous fluid past a nonlinearly stretched plate was conducted by Vajravelu [20]. The fourth-order Runge–Kutta integration approach was used in the solution of his problem. It was found that the heat flow moves from the stretching plate towards the fluid. The influence of Hall current and heat radiation on thermal and mass transportation of a chemically reacting MHD flow of a micropolar fluid over a permeable sheet was studied by Oahimire and Olajuwon [21]. They applied perturbation scheme in order to solve the dimensionless equations. Their results indicated that a rise in the strength of magnetic field leads to a fall in the fluid motion in the direction of the sheet. Recently, hydromagnetic stream and thermal problems have received important motivation at a high level. Thus, the analysis of the effect of hall current, chemical reaction and radiation on a natural convective flow confined by a vertical medium immersed in a spongy surface due to the influence of unvarying magnetic field was scrutinized by Tavva et al. [22]. They applied the simple perturbation method in solving the problem. Their findings showed that both velocity and concentration surges as a result of multiplicative reactions and declines due to a destructive reaction.

Similarly, Kumar et al. [23] considered the impact of Hall current, radiation, Soret as well as Dufour numbers on an unsteady MHD free convection flow through an infinite vertical stationary sheet in an absorbent media. The solution of the dimensionless equations with the boundary constraints were made possible by utilizing the Galerkin technique. It was observed that as the Soret factor enhances, the concentration distribution improves and opposite movement was noticed in terms of Dufour parameter. Accordingly, Cortell [24] performed a numerical examination in line with the boundary layer flow prompted in a quiescent fluid due to continuous plate stretching as a result of the velocity $u_w = (x) \sim x^{\frac{1}{3}}$ in the presence of thermal transfer. The Runge-Kutta fourth order scheme and shooting method were used in solving the problem. From the result, the temperature rises as the temperature ratio number increase and it depreciates as thermal radiation factor improves. The investigative analysis of heat and mass distribution impact on the flow past a stretching sheet with thermal source was investigated by Barik et al. [25]. The solution was carried out by applying Kummer's function. It was noted that tougher suction bound with magnetic field interaction led to a decline in the skin friction coefficient.

In the course of reviewing the above literatures, it's obvious that there's a short fall in analysing the impartation of viscosity degeneracy, absorbent medium and suction numerically on a fluid flow over a non-static wedge. Therefore, we shall take the afore-mentioned flow characteristics into account in this present study. Meanwhile, this work is organised into 5 parts starting with the introduction which contains the significance of the current analysis and review of other studies as the first part. In part 2, the mathematical models of the problem under consideration and the flow arrangement was formulated and presented while part 3 consists of the methodology applied in the solution process and part 4 depicts the gained results and their discussion, followed by the conclusion.

2. FORMULATION OF PROBLEM AND BASIC MODELS

An incompressible, steady laminar hydrodynamic conducting fluid movement over a wedge is appropriated. The coordinated systems due to the $x-axis$ corresponding to the wedge wall is positioned while the normal is along $y-axis$, with constant pressure, p. However, there's an indented angle in tune with the wedge external surface as depicted in figure 1, where
$\alpha = wedge\ angle$. The wall and neighbourhood temperatures of the wedge refers to T_s and T_∞. respectively.

Hence, the following deductions ensue:

- An electrically conducting steady fluid stream equation is provided.
- Impression of degeneracy, porosity with radiative energy is reasoned.
- A constant pressure, p is considered.

In the light of the Boussineq estimate and conditions, the mathematical models of the flow emerges: 2.1

Continuity Equation

$$\frac{\partial u'}{\partial x'} + \frac{\partial v'}{\partial y'} = 0 \tag{1}$$

2.2 Momentum equation

$$u'\frac{\partial u'}{\partial x'} + v'\frac{\partial v'}{\partial y'} = \vartheta\frac{\partial^2 v'}{\partial y'^2} + \frac{v}{k'}u' - \frac{1}{\rho}\frac{\partial p'}{\partial x'} + g\alpha_T(T' - T'_\infty)l^2 \tag{2}$$

2.3 Energy conservation equation

$$u'\frac{\partial T'}{\partial x'} + v'\frac{\partial T'}{\partial y'} = \frac{\mu}{\rho c_p}\frac{\partial^2 T'}{\partial y'^2} + \frac{\mu}{\rho c_p}(T' - T'_\infty) - \frac{k'}{\rho c_p}\frac{\partial qr}{\partial y'} \tag{3}$$

With wall restrictions stated as

$$\left.\begin{aligned} u = U_w = bx^n,\ v = -m,\ T' = T'_s,\ C' = C'_s \quad & \text{at } y = 0 \\ u \to 0,\ T' \to T'_\infty,\ C' \to C'_\infty \quad & \text{as } y \to \infty \end{aligned}\right\} \tag{4}$$

The similarity transformation characteristics include:

$$\eta = y\sqrt{\frac{b(n+1)}{2v}}x^{\frac{(n-1)}{2}}, \quad u = bx^n f'(\eta),\ T' - T'_\infty = (T'_s - T'_\infty)\theta(\eta) \tag{5}$$

$$v = -\sqrt{\frac{bv(n+1)}{2}}\ x^{\frac{n-1}{2}}\left[f(\eta) + \left(\frac{n-1}{n+1}\right)\eta f'(\eta)\right] \tag{6}$$

Where,
$e_0 > 0$ and $e_0 < 0$ are suggestive of suction and injection accordingly. Meanwhile, equation (1) stands for the non-compressible steady continuity equation and equation (2) defines the fluid momentum equation. Equation (3) establishes that heat drift in the fluid takes place in view of convection, reaction

of viscous dissipation and radiative flux, as represented by the first, second and third terms respectively on the right-hand side.

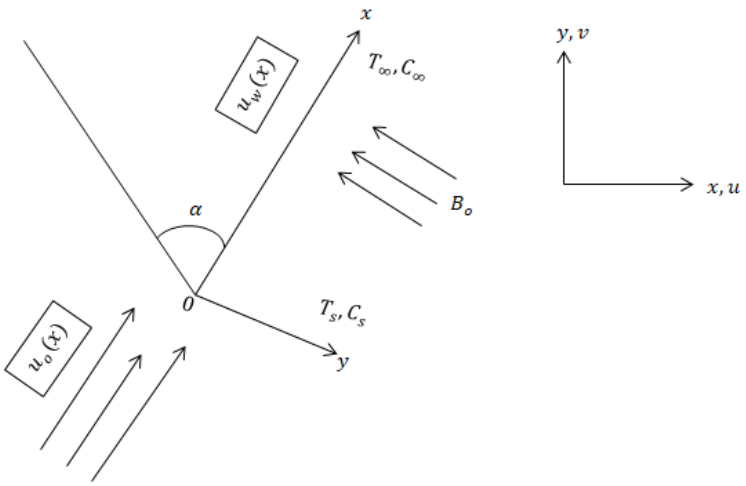

Figure 1. Physical representation of wedge flow

From the relation above, we have l, g as characteristics length and acceleration regarding gravity. Also, the following terms $\vartheta, \rho, C_p, q_r, k, \sigma, p, T, x\ and\ y$ are dynamic velocity, density, capacity of heat, thermal radiative flux, permeability constant, electrical conductivity, pressure, fluid temperature, direction of axes of the velocity components with $u = \frac{\partial \psi}{\partial y}$, $v = -\frac{\partial \psi}{\partial x}$.

3. SOLUTION APPROACH

By adopting the approximation of Rosseland equalities [27] in case of radiation, with

$$q = -\left(\frac{4\sigma^*}{3m_*}\right)\frac{\partial T'^4}{\partial y} \tag{7}$$

With

$\sigma^* \approx 1.3806 \times 10^{-23}$ as Stefan-constant term, $m_* =$ average absorption quantity. Taking the expansion of T^4 about T_∞ in terms of Taylor's series gives

$$T^4 = T_\infty^4 + 3T_\infty^3(T - T_\infty) + 6T_\infty^2(T - T_\infty)^2 + \cdots \tag{7a}$$

Ignoring terms in greater index produces

$$T^4 \cong 4TT_\infty^3 - 3T_\infty^4 \tag{8}$$

Noting that

$$\frac{\partial p'}{\partial x'} = 0 \tag{9}$$

Similarly, using equations (7) – (8) into equation (3) simplifies to

$$u'\frac{\partial T'}{\partial x'} + v'\frac{\partial T'}{\partial y'} = \frac{\mu}{\rho c_p}\frac{\partial^2 T'}{\partial y'^2} + \frac{\partial^2 T'}{\partial y'^2}\frac{16\sigma^* T_\infty^3}{3m_f^*} + \frac{\mu}{\rho c_p}(T' - T'_\infty) \tag{10}$$

Transformation of equations (2), (4) and (10) with the non-dimensional variables in equations (5) and (6) assumes

$$\frac{d^3f}{d\eta^3} + f(\eta)\frac{d^2f}{d\eta^2} + Kr\frac{df}{d\eta} + Gl\theta(\eta) = 0 \tag{11}$$

$$\frac{d^2\theta}{d\eta^2}(1 + Nr) + Prf(\eta)\frac{d\theta}{d\eta} + PrEc\theta(\eta) = 0 \tag{12}$$

$$\frac{df}{d\eta} = 1,\ f(\eta) = m_o, \theta(\eta) = 1 \qquad \text{at } \eta = 0 \tag{13}$$

$$\frac{df}{d\eta} \to 0, \qquad \theta(\eta) \to 0 \qquad \text{as } \eta \to \infty \tag{14}$$

Where,

$K = \frac{k'v_o^2}{v^2}$, $A = \frac{16\sigma^* T_\infty^3}{3k^* k}$, $Pr = \frac{\mu C_p}{k}$, $Ec = \frac{u^2}{C_p \Delta T} \ni \Delta T = T_s' - T_\infty'$, $Gl = \frac{\alpha_T l^2 g(T_s - T_\infty)}{uv}$, specify the Porosity, radiation, Prandtl, Eckert and local thermal Grashof relations.

3.1. Analytical Solution

The analytical solution of the problem has been carried out by utilizing the regular perturbation method. It is a mathematical technique used to obtaining approximate solutions for differential equations that contain a small parameter, say Γ. This technique is mainly useful when the differential equation is coupled, difficult or impossible to be solved directly but can be simplified by assuming that the small parameter Γ is much smaller than 1.

Step 1: We need to state or write down an ordinary differential equation involving a small parameter Γ.
Step 2: We assumed that the solution can be expressed as a power series in terms of the small parameter Γ: i.e., $y(\eta) = y_0(\eta) + \Gamma y_1(\eta) + \Gamma^2 y_2(\eta) + \cdots$ (15)
where $y_0(\eta), y_1(\eta), y_2(\eta)$, etc., are functions that are to be determined.
Step 3: We substituted the assumed solution into the original ODE in order to obtain a series of equations.
Step 4: We equated coefficients of different powers of Γ, so as to generate a set of equations involving the unknown functions $y_0(\eta), y_1(\eta), y_2(\eta)$, etc. These equations were solved to determine the expressions for the unknown functions.
Step 5: As soon as the expressions for $y_0(\eta), y_1(\eta), y_2(\eta)$, etc., were found, we substituted them into the assumed solution of equation (15) to realize the approximate solution, $y(\eta)$.
Step 6: We applied the boundary conditions (given) to determining the integration constants that appeared in the solutions obtained in Step 4 above.
Relating to Bestman [28], we have

$$\eta = \Delta e_0, \quad f(\eta) = e_0 F(\eta), \quad \theta(\eta) = \varphi(\eta), \quad \Gamma = \frac{1}{{e_0}^2} \tag{16}$$

Inputting equation (16) and its differentials into equations (11) – (12) produces,

$$\frac{d^3f}{d\eta^3} + f(\eta)\frac{d^2f}{d\eta^2} + \Gamma K\frac{df}{d\eta} + \Gamma^2 Gl\varphi(\eta) = 0 \tag{17}$$

$$\frac{d^2\varphi}{d\eta^2}(1 + Nr) + Prf(\eta)\frac{d\varphi}{d\eta} + \Gamma\varphi(\eta)PrEc = 0 \tag{18}$$

Which depends on:

$$\left.\begin{aligned} \eta = 0; \quad f = 1,\ \frac{df}{d\eta} = e_0,\ \varphi = 1 \\ \eta \to \infty;\ \frac{df}{d\eta} \to 0, \qquad h \to 0 \end{aligned}\right\} \tag{19}$$

The application of the regular perturbation technique in resolving equations (17) and (18) follows. Thus, let the series solution be:

$$f(\eta) = 1 + \sum_{k=n=1}^{\infty} (\Gamma)^k f_n(\eta) \quad (20)$$

$$\varphi(\eta) = \sum_{k=n=1}^{\infty} (\Gamma)^k \varphi_n(\eta) \quad (21)$$

Differentiating equations (20) trice and (21) twice in terms of η, using the results in equations (17) – (18) and simplifying, shows that at zeroth order, we have:

$$\frac{d^2\varphi_o}{d\eta^2}(1 + Nr) + Pr\frac{d\varphi_o}{d\eta} = 0: \varphi_o(0) = 1, \varphi_o(\infty) = 0 \quad (22)$$

Evaluating at order one (1) provides:

$$\frac{d^3 f_1}{d\eta^3} + \frac{d^3 1}{d\eta^3} = 0: f_1(0) = 0, f_1'(0) = 1, \ f_1'(\infty) = 0 \quad (23)$$

$$\frac{d^2\varphi_1}{d\eta^2}(1 + Nr) + Pr\frac{d\varphi_1}{d\eta} + Prf_1(\eta)\frac{d\varphi_o}{d\eta} + EcPr\varphi_o(\eta) = 0: \varphi_1(0) = 0, \varphi_1(\infty) = 0 \quad (24)$$

In terms of order two (2), we gained

$$\frac{d^3 f_2}{d\eta^3} + \frac{d^3 f_2}{d\eta^3} + f_1(\eta)\frac{d^2 f_1}{d\eta^2} + K\frac{df_1}{d\eta} + Gl\varphi_o(\eta) = 0: f_2(0) = 0, f_2'(0) = 0, f_2'(\infty) = 0 \quad (25)$$

The analytical solutions mentioned below are obtained by solving equations (22) – (25) in line with their appropriate and respective wall conditions.

$$f'(\eta) = exp - \eta + \frac{1}{(e_o)^2}\left(-\eta exp - \eta - exp - \eta - \frac{1}{2}exp - 2\eta + k\eta exp - \eta + kexp - \eta - \frac{Gl}{j(j-1)}exp - j\eta + S_4 - S_6 exp - \eta\right) \quad (26)$$

$$\varphi(\eta) = exp - j\eta + \frac{1}{(e_o)^2}\left(-j\eta exp - j\eta - \frac{(j)^2}{1+j}exp - (1+j)\eta + Ec\eta exp - j\eta + \frac{(j)^2}{1+j}exp - j\eta\right) \quad (27)$$

With,

$S_4 = 0, S_6 = k - \frac{3}{2} - \frac{Gl}{j(j-1)}, j = \frac{Pr}{1+A}$ as the constants.

Nonetheless, in the engineering designing of various forms of devices, the Nusselt number, Nu which represents the rate at which thermal energy is conveyed through a given scheme, becomes very relevant. Thus,

$$Nu = \varphi'(\eta) = -(1 + A)\left(\frac{\partial\varphi}{\partial\eta}\right)_{\eta=0} \quad (28)$$

3.2. Numerical Simulation

The Mathematica scheme and Wolfram language have been applied to finding the numerical results of equations (26) – (28) respectively. Hence, such solutions are offered in form of graphs containing legends as demonstrated below.

4. RESULTS AND DISCUSSION

From the graphical results, $f'(\eta)$ and $\varphi(\eta)$ implies velocity and temperature of flowing fluid and represents the vertical axis while the independent variable, η is on the horizontal axis.

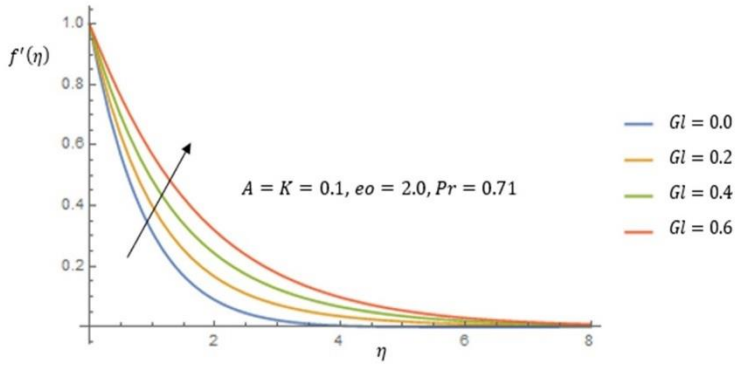

Figure 2. Influence of local thermal Grashof parameter, Gl on the fluid flow rate

In Figure 2, as the dominance of the buoyancy force proportion overshadows the viscous force, the flow field rises. Thus, the flow rate $f'(\eta)$, heightens as the dimensionless fluid parameter values of Gl increases. The result of varying the values of radiation A in ascending array, on the momentum and temperature of the moving fluid is visualized in Figures 3 and 4, accordingly. However, the introduction of this parameter (A) into the flow, changes heat energy into kinetic form and as it augments continually, both $f'(\eta)$ and $\varphi(\eta)$ intensifies.

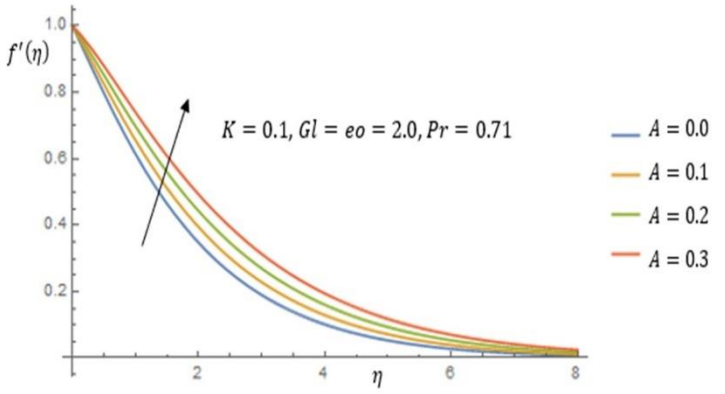

Figure 3. Influence of radiation constraint, A on the fluid flow rate

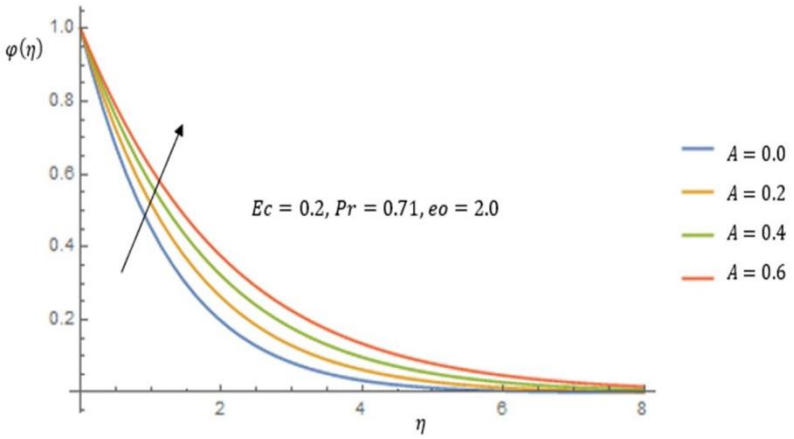

Figure 4. Influence of radiation number, A on the energy transmission rate

The impact of the permeability factor, k is explained in Figure 5. Meanwhile, due to the spongy nature of the medium through which the fluid flow takes place, the rate of tide changes dynamically resulting to a surge in momentum boundary layer. Thus, the upsurge in the values of k, leads to an appreciable enhancement in the flow distribution of $f'(\eta)$.

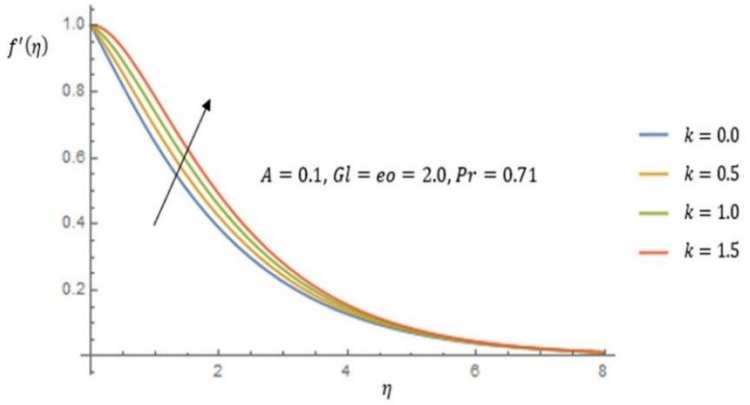

Figure 5. Influence of porosity constraint, k on the fluid flow rate

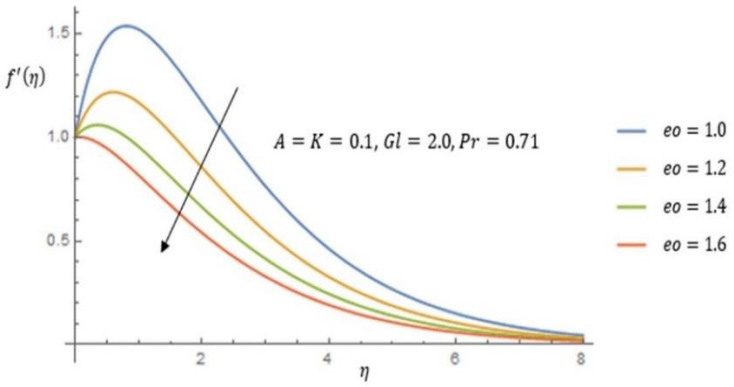

Figure 6. Influence of suction constraint, e_o on the fluid flow rate

Similarly, the development of $f'(\eta)$ and $\varphi(\eta)$ owing to the effects of suction parameter, eo on fluid rate and thermal transfer are depicted in Figures 6 and 7 respectively. Whence, raising the values of this parameter informs increasing speed of fluid motion, $f'(\eta)$ and thermal boundary layer with a rising field of $\varphi(\eta)$.

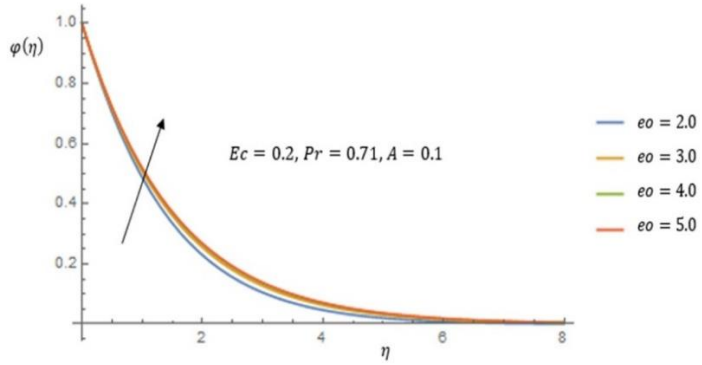

Figure 7. Influence of suction number, e_o on the energy transmission rate

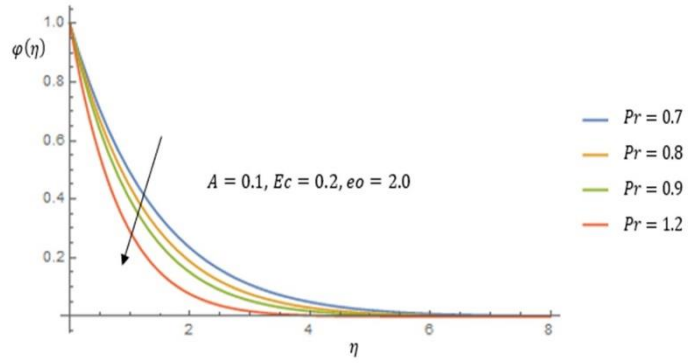

Figure 8. Influence of Prandtl factor, Pr on the energy transmission rate

Figure 8, captures the result of the uprising effect of Pr on temperature. Meanwhile, the ratio of viscous to thermal diffusivity rate is referred to as Prandtl factor. Therefore, as a non-dimensional number, when $Pr \ll 1$, the thermal boundary layer thickness becomes bigger when compared with $Pr \gg 1$. Therefore, improving the values of Pr reflects a fall in $\varphi(\eta)$.

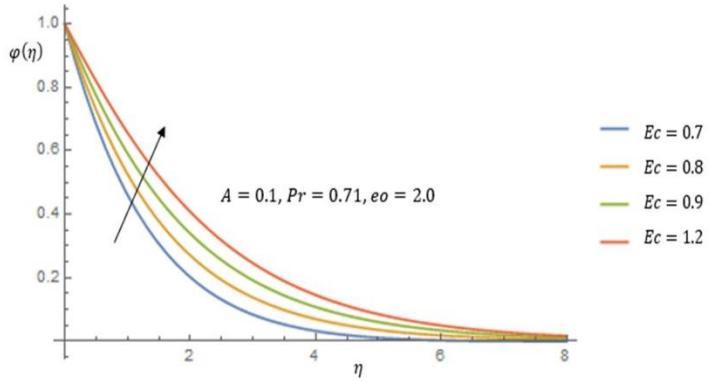

Figure 9. Influence of Eckert constraint, Ec on the energy transmission rate

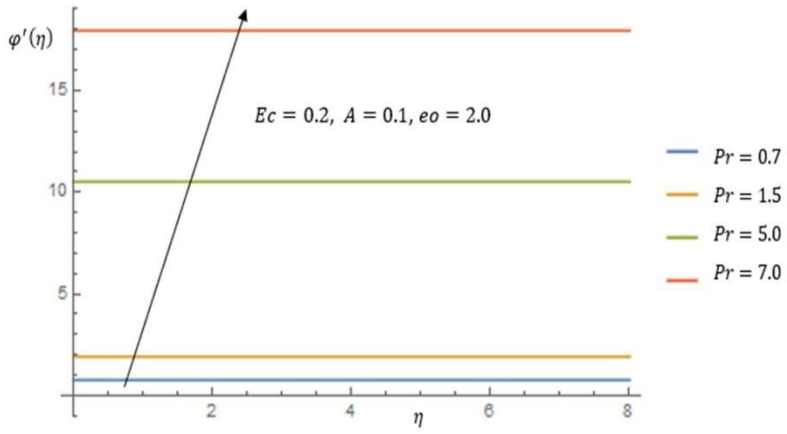

Figure 10. Influence of Pr on Nusselt number, Nu

In Figure 9, the influence of Eckert constraint, Ec on $\varphi(\eta)$ of fluid stream is obvious. The dimensionless number, Ec relates to the connection concerning the flow's energy kinetically with energy variance existing at the wall in terms of debauchery through heat transference. Thus, appreciating values of Ec embraces increment in the fluid's temperature, $\varphi(\eta)$. The stimulus as a result of enhancing values of Pr

on Nu, is referenced in Figure 10. When Pr < 1, heat spreads slowly but at Pr > 1, the rate of thermal transference intensifies as shown in Table 1 below and the above mentioned Figure 10. Thus, growing values of Pr aids in regulating the speed at which a conducting fluid cools in a given system. Therefore, heat disperses quickly thereby helping to guide the temperature of a given device functioning with the dynamics of fluid flow in several physical applications. However, the evolving changes on thermal transmission rate, (Nu) as a result of increasing values of A are highlighted in both Table 2 and Figure 11. Nevertheless, from these two forms of data presentations, it can be detected that as A improves, the rate of heat conveyance, (Nu) recedes.

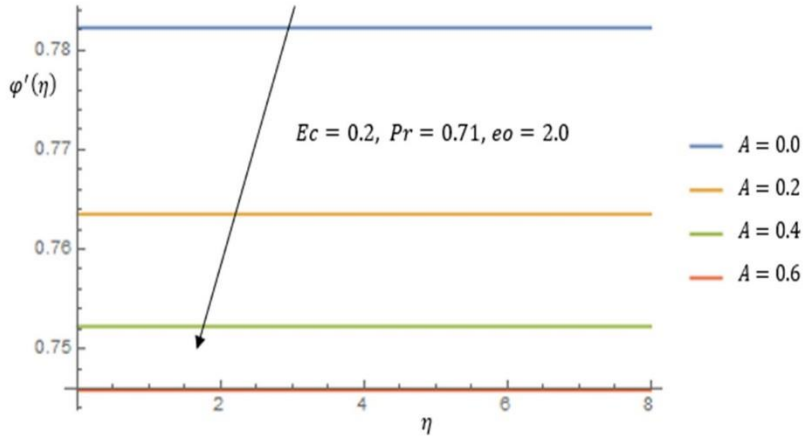

Figure 11. Influence of A, on Nusselt number, Nu

Table 1. Nusselt number coefficient for varying values of Pr at $e_o = 2.0$

A	Ec	Pr	$-\varphi'(0)$
0.1	0.2	0.7	0.7594
0.1	0.2	1.5	1.9077
0.1	0.2	5.0	10.5114
0.1	0.2	7.0	17.9537

Table 2. Nusselt number coefficient for varying values of A at $e_o = 2.0$

A	Ec	Pr	$-\varphi'(0)$
0.0	0.2	0.71	0.7822
0.2	0.2	0.71	0.7635
0.4	0.2	0.71	0.7523
0.6	0.2	0.71	0.7458

5. CONCLUSION

The analysis of the influence of viscous degeneracy for the augmentation of thermal transferal over a moving wedge in a porous domain is deliberated. From the results obtained by means of using perturbation approach and an in-built Wolfram Mathematica solver, the following concluding remarks are made.
(a) The momentum boundary layer increases as Gl and k improves in their values, thus leading to upsurge in the fluid velocity.
(b) There is an increase in the fluid's velocity, $f'(\eta)$ and temperature, $\varphi(\eta)$ as the values of radiation A and suction eo parameters enhances.
(c) Increasing values of Ec raises the thermal wall layer such that $\varphi(\eta)$ of the fluid grows while the reverse is the condition when Pr improves.
(d) The rate of heat transfer, Nu is brought under control through cooling when Pr intensifies whereas for A, the opposite is the outcome.
Meanwhile, in line with the current study, the suggestive areas of future research include numerical simulations and optimization techniques: Thus, the conduction of advanced numerical simulations using Computational Fluid Dynamics (CFD) and optimization procedures to study the fluid flow and heat transfer characteristics over a moving wedge in a porous chamber due to viscous dissipation remains a future research area to be explored. Also, the investigation of diverse geometries, permeability distributions, and wedge motion patterns to optimize the heat transfer performance and identify the most efficient configuration, forms another area of future research.

CONFLICT OF INTEREST

We state that there are no conflicts of interest of any type as regards to the publication of this article.

ACKNOWLEDGEMENT

We wish to appreciate the referees for their constructive input towards the improvement of this study.

AUTHORSHIP CONTRIBUTIONS

Conceiving and designing of the research study by Uchenna Awucha Uka[1]; Contributions to the theoretical framework of the research through the provision of critical intellectual input throughout the research process by Uchenna Awucha Uka[1], Innocent Chukwuemeka Emeziem[2], Semiu Akinpelu Ayinde[3], Charles Adenika[3], Kelvin Onyekwere Agbo[3]; Solution of the transformed mathematical model by Uchenna Awucha Uka[1], Innocent Chukwuemeka Emeziem[2] and Charles Adenika[3]; Contributions on result analysis, interpretation of results, participation in the revision and formatting of the research manuscript by Uchenna Awucha Uka[1], Innocent Chukwuemeka Emeziem[2], Semiu Akinpelu Ayinde[3], Charles Adenika[3], Kelvin Onyekwere Agbo[3]; Provision of subject matter expertise, reviewed and revised the manuscript for clarity and scientific rigor and ensured adherence to ethical considerations by Uchenna Awucha Uka[1] and Innocent Chukwuemeka Emeziem[2]; Re-checking of the article not only for spelling and grammar but also for intellectual content before submission by Uchenna Awucha Uka[1], Innocent Chukwuemeka Emeziem[2], Semiu Akinpelu Ayinde[3], Charles Adenika[3], Kelvin Onyekwere Agbo[3].

Supervision of the overall research project and provision of guidance throughout the research process by Uchenna Awucha Uka[1]; Also, all the authors played a significant role in the manuscript revision and its final approval.

Therefore, all the authors have read and approved the final version of the manuscript and have agreed to its submission for publication.

REFERENCES

[1] Falkner VM, Skan SW. Solutions of the boundary layer equations. Philosophical Magazine 1931; 7: 865-896.

[2] Fang T, Yao S, Zhang J, Zhang Y, Tao H. Momentum and heat transfer of the Falkner-Skan flow with algebraic decay: an analytical solution. Commun. Nonlinear Sci. Numer Simul 2012; 17(6): 2476-2488.

[3] Ashraf M, Narahari M, Muthuvalu MS. Mixed convection flow over a stretching porous wedge with Newtonian heating in the presence of heat generation or absorption. In: AIP Conference Proceedings 2016; 1787, 020004, AIP, New York.

[4] Ahmad K, Hanouf Z, Ishak A. MHD Casson nanofluid flow over a wedge with Newtonian heating. Eur. Phys. J. Plus 2017; 132(2): 87.

[5] Hossain M, A Roy NC, Siddiqa S. Unsteady mixed convection dusty fluid flow over a vertical wedge with small fluctuation in free stream and surface temperature. Appl. Math. Comput 2017; 293: 480-492.

[6] Shit GC, Majee S. Hydromagnetic flow past an inclined nonlinear spreading material with fickle viscosity in the presence of thermal radiation and chemical reaction. Journal of Applied Fluid Mechanics 2014; 7(2): 239-247.

[7] Rahman MM, Al-Lawatia MA, Eltayeb AI, Al-Salti N. Hydromagnetic slip flow of water based nanofluids past a wedge with convective surface in the presence of heat generation/absorption. International Journal of Thermal Sciences 2012; 57: 172-182.

[8] Sulochana G, Ashwinkumar GP, Sandeep N. Effect of frictional heating on mixed convection flow of chemically reacting radiative Casson nanofluid past an inclined porous plate. Alex. Eng J 2018; 57(4): 2573-2584. https://doi.org/10.1016/j.aej.

[9] Ashwini G, Eswara AT. MHD Falkner-Skan boundary layer flow with internal heat generation or absorption . World Academy of Science, Engineering and Technology 2012; 65: 662-665.

[10] Khan WA, Pop I. Boundary layer flow over a wedge passing in a nanofluid. Mathematical Problems in Engineering 2013; 637-285.

[11] Yacob NA, Ishak A, Nazar R, Pop I. Falkner-Skan problem for a static and moving wedge with prescribed surface heat flux in a nanofluid. International Communications in Heat and Mass Transfer 2011; 38: 149-153.

[12] Chamkha AJ, Abbasbandy S, Rashad AM, and Vajravelu K. Radiation effects on mixed convection over a wedge immersed in a permeable medium filled with a nanofluid. Transport in Porous Media 2012; 91: 261-279.

[13] Kasmani RM, Muhaimin I, Kandasamy R. Laminar boundary layer flow of a nanofluid along a wedge in the presence of suction/injection. Journal of Applied Mechanics and Technical Physics 2013; 54(3): 377-384.

[14] Ullah I, Bhattacharyya K, Shafie S, Khan I. Unsteady MHD mixed convection slip flow of Casson fluid past nonlinearly stretching sheet embedded in a porous medium with chemical reaction,

thermal radiation, heat generation/absorption and convective boundary conditions. Public Library of Science One (PLoS ONE) 2016; 10(11) http://doi.org/10.1371/journal.pone.0165348.

[15] Aman S, Khan I, Ismail Z, Salleh MZ. Impacts of gold nanoparticles on MHD mixed convection Poiseuille flow of nanofluid passing through a porous medium in the presence of thermal radiation, thermal diffusion and chemical reaction. Naural Computing and Applications 2016; 30(3): 14 789-797.

[16] Ahmed N, Khan U, Mohyud ST. Influence of an effective Prandtl number model on squeezed flow of $\gamma AL2O3 - H2O$ and $\gamma AL2O3 - C2H6O2$ nanofluids. Journal of Molecular Liquids 2017; 238: 447- 17 454.

[17] Adnan M, Asadullah M, Khan U, Ahmed N, Mohyud-Din ST. Analytical and Numerical investigation of thermal radiation effects on flow of viscous incompressible fluid with stretchable convergent/divergent channels, Journal of Molecular Liquid 2016; 224: 768-775.

[18] Ullah K, Bhattacharyya K, Shafie S. Hydromagnetic Falkner-Skan flow of Casson fluid over a moving wedge due to heat transfer. Alexandria Engineering Journal 2016; 55(3): 2139-2148.

[19] Khan AW, Pop I. Math. Prob. Eng 2013; 1-7.

[20] Vajravelu K. Viscous flow over a nonlinearly stretching plate. Applied Mathematics and Computation 2001; 124(3): 281-288.

[21] Oahimire, JI, Olajuwon BI. Effect of Hall current and thermal radiation on heat and mass transfer of a chemically reacting MHD flow of a micropolar fluid past a porous medium. Journal of King Saud University-Engineering Sciences 2013; 1-10. http://dx.doi.org/10.1016/j.jksues.2013.06.008.

[22] Tavva SR, Reddy OSP, Raju MC, Varma SVK. MHD free convection heat and mass transfer flow through a porous medium bounded by a vertical surface in the presence of hall current. Advances in Applied Science Research 2012; 3(6): 3482-3490.

[23] Kumar MA, Reddy YD, Goud BS, Rao VS. Effects of Soret, Dufour, Hall current and radiation on MHD natural convective heat and mass transfer flow past an accelerated vertical plate through a porous medium. International Journal of Thermofluids 2021; 9: 100061. https://doi.org/10.1016/j.ijft.2010100061.

[24] Cortell R. Fluid flow and radiative nonlinear heat transfer over a stretching sheet. Journal of King Saud University-Engineering Sciences 2014; 26: 161-167. https://dx.doi.org/10.1016/j.jksus.2013.08.004.

[25] Barik RN, Dash GC, Rath PK. Heat and mass transfer on MHD flow through a porous medium over a stretching surface with heat source. Mathematical Theory and Modeling 2012; 2(7): 49-59.

[26] Boussinesq J. Analytical Theory of Heat. Gauthier-Villars. Paris, 1877.

[27] Rosseland S. Theoretical Astrophysics. Clarendon Press, Oxford, 1936.

[28] Bestman AR. The boundary-layer flow past a semi-infinite heated porous plate for two-component plasma. Astrophysics and Space Science 1990; 173: 93-100.

ESKİŞEHİR TECHNICAL UNIVERSITY JOURNAL OF SCIENCE AND TECHNOLOGY
A- APPLIED SCIENCES AND ENGINEERING

2023, 24(3), pp. 177-191, DOI:10.18038/estubtda.1312725

RESEARCH ARTICLE

Q-HOMOTOPY SHEHU ANALYSIS TRANSFORM METHOD OF TIME-FRACTIONAL COUPLED BURGERS EQUATIONS

Umut BEKTAŞ [1] **Halil ANAÇ** [2,*]

[1] Department of Mathematical Engineering, Faculty of Natural Sciences and Engineering, Gumushane University, Gumushane, Turkey
[2] Department of Computer Technologies, Torul Vocational School, Gumushane University, Gumushane, Turkey

ABSTRACT

In this study, numerical solutions to time-fractional coupled Burgers equations are obtained utilizing the q-homotopy Shehu analysis transform method. The definition of fractional derivatives in the sense of Caputo. q-homotopy Shehu analysis transform method is also used to find the numerical solutions of the time-fractional coupled Burgers equations. In addition, the MAPLE software is utilized to plot the graphs of the solutions. These results demonstrate that the presented method is accurate and simple to implement.

Keywords: q-homotopy Shehu analysis transform method, Coupled Burgers equations, Mittag-Leffler function

1. INTRODUCTION

Fractional differential equations (FDEs) have recently gained popularity in numerous scientific areas. [1-6]. The fractional technique is commonly utilized to simulate a variety of difficulties, and it is widely applied to numerous problems in mechanics, anomalous diffusion, wave propagation, and turbulence, among others [7-9]. Thus, numerous scientists research fractional calculus extensively and work to enhance it. One of the greatest benefits of utilizing FDEs with non-local properties is that they display novel properties for several difficulties. Nonlinear FDEs are challenging to solve for a variety of reasons. Because the majority of FDEs isn't be solved analytically, efficient and potent numerical approaches are devised. But the numbers of the approaches are fairly limited.

However, the fractional order varies based on time and space. The scenario leads to a rapidly expanding field of FPDEs with fractional operators of variable order [10-19]. Several potent numerical approaches were established in the scientific literature, and numerous eminent scholars contributed to this topic. Several of these techniques include the adomian decomposition method (ADM) [20], homotopy perturbation method (HPM) [21-23], homotopy analysis method (HAM) [24-25], the collocation method [26-31], the Sumudu transform method (STM) [32-33], the differential transform method (DTM) [34-38].

For analyzing differential equations in the time domain, the Shehu transform, a generalization of the Laplace and Sumudu integral transforms, is introduced [39]. Iterative Shehu transform method (ISTM) is developed, which leverages the Shehu transform (ST) approach and decomposes the nonlinearity component to create a simple and effective solution for solving FPDEs [40]. A two-dimensional version of the one-dimensional Shehu transform is developed [41]. The fuzzy Shehu transform technique (FSTM) is presented by employing Zadeh's decomposition theorem and fuzzy Riemann integral of real-valued functions on finite intervals [42]. Using the natural transform decomposition technique and the iterative Shehu transform method with a singular kernel derivative, the time-fractional Klein-Gordon

*Corresponding Author: halilanac0638@xgmail.com
Received: 10.06.2023 Published: 22.09.2023

equation was studied [43]. To solve time-fractional gas dynamics equations, the variational iteration transform method is combined with ST and VIM [44]. By using the established q-Shehu transform, the solutions of the q-fractional kinetic equations are found in terms of the constructed generalized hyper-Bessel function [45]. The notion of ST in q-calculus, q-Shehu transform, is introduced along with its features [46].

The time-fractional coupled Burgers equation is [47]

$$\begin{cases} \dfrac{\partial^{\alpha}u}{\partial\tau^{\alpha}} + u\dfrac{\partial u}{\partial\zeta} + w\dfrac{\partial u}{\partial\mu} = \dfrac{1}{Re}\left[\dfrac{\partial^{\alpha}u}{\partial\zeta^{\alpha}} + \dfrac{\partial^{\alpha}u}{\partial\mu^{\alpha}}\right], \\ \dfrac{\partial^{\beta}w}{\partial\tau^{\beta}} + u\dfrac{\partial w}{\partial\zeta} + w\dfrac{\partial w}{\partial\mu} = \dfrac{1}{Re}\left[\dfrac{\partial^{\beta}w}{\partial\zeta^{\beta}} + \dfrac{\partial^{\beta}w}{\partial\mu^{\beta}}\right], 0 < \zeta, \mu < 1, \qquad 0 < \alpha, \beta < 1, \tau > 0. \end{cases} \tag{1}$$

The Burgers model of turbulence is an extremely influential fluid dynamics model. Various scientists have contemplated examining the theory and model of shock waves in order to get theoretical knowledge of a physical flow class and to assess various approximation approaches. Eq. (1) has the advantage over competing numerical formulations of viscous diffusion and nonlinear advection in that it is the simplest. It illustrates the fundamental forms of the dissipation term $w\frac{\partial u}{\partial\mu}$ and the nonlinear advection term $u\frac{\partial u}{\partial\zeta}$, where Re is the Reynolds number that is used to model the naturally occurring phenomena of wave motions and hence determine the behavior of the solution. Cole [48] examined the mathematical characteristics of Equation (1). In physics and applied mathematics, nonlinear phenomena play a significant role. The significance of getting actual or estimated outcomes of PDEs in science in terms of exploring new strategies; this is still a popular topic [49–52]. Utilizing nonlinear PDEs, a variety of strategies for obtaining the real results of the numerous physical models presented have been proposed. Bateman [53] created a notable model and identified its consistent results, that are illustrative of numerous viscous flows. Later, Burgers [48] proposed it as one of the class models describing mathematical turbulence problems. It was described by Hopf [54] in gas dynamics. In addition, they demonstrated separately that the Burgers equation may be solved for any initial condition. Numerical solutions for the one-dimensional Burgers equation was investigated [55]. Nonlinear convection and the viscosity terms unquestionably chasten the Navier–Stokes equation [56-57].

This article aims to introduce a new method, the q-homotopy Shehu analysis transform method, and to use it to get new numerical solutions for coupled Burgers equations.

The remainder of the study is detailed below. In Section 2, fundamental fractional derivative definitions and the Shehu transform of fractional derivatives are provided. In Section 3, q-homotopy Shehu analysis transform method is provided. In Section 4, the numerical solutions of the time-fractional coupled Burgers equations are presented. Section 5 introduces the conclusion.

2. PRELIMINARIES

Several fundamental definitions are provided in the part.

Definition 1 [4, 58-59]. The Riemann-Liouville fractional integral is described as

$$I^{a}f(x) = \begin{cases} \dfrac{1}{\Gamma(a)}\displaystyle\int_{0}^{x}(x-t)^{a-1}f(t)dt\,, \quad a > 0, x > 0, \\ I^{0}f(x) = f(x), \qquad a = 0. \end{cases} \tag{2}$$

Definition 2 [4, 58-59]. The Caputo fractional derivative (CFD) is given by

$$D^a f(x) = I^{a-n} D^n f(x) = \frac{1}{\Gamma(n-a)} \int_0^x (x-t)^{n-a-1} f^{(n)}(t) dt, \quad (3)$$

where $n-1 < a \leq n,\ n \in N,\ x > 0, f \in C_{-1}^n$.

Definition 3 [12]. The Mittag-Leffler function $\boldsymbol{E_a}$ is defined as

$$E_a(z) = \sum_{n=0}^{\infty} \frac{z^a}{\Gamma(na+1)}, a > 0. \quad (4)$$

Definition 4 [39]. The Shehu transform (ST) of the function $f(t)$ is given by

$$\mathrm{S}[f(t)] = V[s,u] = \int_0^{\infty} f(t) e^{-\frac{st}{u}} dt, s > 0, u > 0. \quad (5)$$

Definition 5 [39]. If $\mathrm{V}(s,u)$ is the ST of the function $f(t)$, then ST of CFD is defined by

$$\mathrm{S}[D^{\alpha} f(t)] = \left(\frac{\mathrm{S}}{\mathrm{u}}\right)^{\alpha} \mathrm{V}(s,u) - \sum_{k=0}^{n-1} \left(\frac{\mathrm{S}}{\mathrm{u}}\right)^{\alpha-k-1} f^{(k)}(0), n-1 < \alpha \leq n. \quad (6)$$

3. THE METHODOLOGY OF q-HOMOTOPY SHEHU ANALYSIS TRANSFORM METHOD

In this part, q-HSATM for nonlinear FPDEs is presented. In order to illustrate the technique for the suggested method, the nonlinear FPDEs are written in standard operator form

$$D_t^a u(x,t) + Au(x,t) + Nu(x,t) = g(x,t), t > 0, n-1 < \alpha \leq n, \quad (7)$$

with the initial condition

$$u(x,0) = h(x), \quad (8)$$

where A is a linear operator, N is a nonlinear operator, $g(x,t)$ is a source term and D_t^a is a time-fractional derivative operator of order α.

Now, by performing Shehu transform on Eq. (7) and using the initial condition, it is acquired as

$$S[u(x,t)] - \sum_{k=0}^{n-1} \left(\frac{\mathrm{S}}{\mathrm{u}}\right)^{-k-1} \frac{\partial^k u(x,t)}{\partial t^k}|_{t=0} + \left(\frac{u}{s}\right)^{\alpha} S[Au(x,t) + Nu(x,t) \quad (9)$$

$$-g(x,t)] = 0. \quad (10)$$

The nonlinear operator by the assist of HAM for real function $\varphi(x,t;q)$ is defined as

$$N[\varphi(x,t;q)\,] = S[\varphi(x,t;q)\,] - \frac{u}{s}\varphi(x,t;q)\,(0^+) + \left(\frac{u}{s}\right)^{\alpha} \{S[Au(x,t) + Nu(x,t) \quad (11)$$

$$-g(x,t)]\}, \quad (12)$$

where $q\epsilon\left[0,\frac{1}{n}\right]$.
It is established a homotopy as follows

$$(1-nq)S\left[\varphi(x,t;q)-\frac{u}{s}\varphi(x,t;q)\ (0^{+})\right]=hqH(x,t)N[\varphi(x,t;q)], \tag{13}$$

where, $h\neq 0$ is an auxiliary parameter and S represents Shehu transform. For $q=0$ and $q=\frac{1}{n}$, the results in Eq. (13) are respectively provided:

$$\varphi(x,t;0)=u_0(x,t),\varphi\left(x,t;\frac{1}{n}\right)=u(x,t), \tag{14}$$

Therefore, by amplifying q from 0 to $\frac{1}{n}$, then the solution $\varphi(x,t;q)$ converges from $u_0(x,t)$ to the solution $u(x,t)$. Employing the Taylor theorem around q and expanding $\varphi(x,t;q)$ and then, it is obtained as

$$\varphi(x,t;q)=u_0(x,t)+\sum_{i=1}^{\infty}u_m(x,t)q^m, \tag{15}$$

where

$$u_m(x,t)=\frac{1}{m!}\frac{\partial^m\varphi(x,t;q)}{\partial q^m}|_{q=0}. \tag{16}$$

Eq. (15) converges at $q=\frac{1}{n}$ for the appropriate $u_0(x,t)$, n and h. Then, we have one of the solutions of the original nonlinear equation of the form

$$u(x,t)=u_0(x,t)+\sum_{m=1}^{\infty}u_m(x,t)\left(\frac{1}{n}\right)^m. \tag{17}$$

If we differentiate the zeroth order deformation Eq. (13) m −times with respect to q and we divide by $m!$, respectively, then for $q=0$, it is obtained as

$$S[u_m(x,t)-k_mu_{m-1}(x,t)]=hH(x,t)\mathcal{R}_m(\vec{u}_{m-1}), \tag{18}$$

where the vectors are defined by

$$\vec{u}_m=\{u_0(x,t),u_1(x,t),\dots,u_m(x,t)\}. \tag{19}$$

When the inverse Shehu transform to Eq. (18) is applied, then it is obtained as

$$u_m(x,t)=k_mu_{m-1}(x,t)+hS^{-1}[H(x,t)\mathcal{R}_m(\vec{u}_{m-1})], \tag{20}$$

where

$$\mathcal{R}_m(\vec{u}_{m-1}) = \mathrm{S}[u_{m-1}(x,t)] - \left(1 - \frac{k_m}{n}\right)\frac{\mathrm{u}}{s}u_0(x,t), \tag{21}$$

$$+\left(\frac{u}{s}\right)^{\alpha}\mathrm{S}\big(Au_{m-1}(x,t) + H_{m-1}(x,t) - \mathrm{g}(x,t)\big), \tag{22}$$

and

$$k_m = \begin{cases} 0, & m \leq 1, \\ n, & m > 1. \end{cases} \tag{23}$$

Here, H_m is homotopy polynomial and presented as

$$H_{m-1} = \frac{1}{(m-1)!}\frac{\partial^{m-1}\varphi(x,t;q)}{\partial q^{m-1}}|_{q=0}, \tag{24}$$

and

$$\varphi(x,t;q) = \varphi_0 + q\varphi_1 + q^2\varphi_2 + \cdots \tag{25}$$

By using Eqs. (20-22), it is obtained

$$u_m(x,t) = (k_m + h)u_{m-1}(x,t) - \left(1 - \frac{k_m}{n}\right)\frac{\mathrm{u}}{s}u_0(x,t) \tag{26}$$

$$+hS^{-1}\left[\left(\left(\frac{u}{s}\right)^{\alpha}\mathrm{S}\big(Au_{m-1}(x,t) + H_{m-1}(x,t) - \mathrm{g}(x,t)\big)\right)\right]. \tag{27}$$

By utilizing q-HSATM, the series solution is defined by

$$u(x,t) = \sum_{i=0}^{\infty} u_m(x,t). \tag{28}$$

3.1. Convergence Analysis of q-HSATM Solutions

Theorem 1 (Uniqueness theorem) [60] The solution for the Eq. (7) obtained by q-HSATM is unique for every $\boldsymbol{\gamma} \in (\mathbf{0}, \mathbf{1})$, where $\boldsymbol{\gamma} = (\boldsymbol{n} + \boldsymbol{h}) + \boldsymbol{h}(\boldsymbol{\epsilon} + \boldsymbol{\alpha})\boldsymbol{T}$.

Theorem 2 (Convergence theorem) [60] Let **X** be a Banach space and $\boldsymbol{F}: \boldsymbol{X} \to \boldsymbol{X}$ be a nonlinear mapping. Assume that

$$\|\boldsymbol{G}(\boldsymbol{a}) - \boldsymbol{G}(\boldsymbol{h})\| \leq \boldsymbol{\gamma}\|\boldsymbol{a} - \boldsymbol{h}\|, \forall \boldsymbol{a}, \boldsymbol{b} \in \boldsymbol{X}, \tag{29}$$

then **G** has a fixed point in view of Banach fixed point theory **[61]**. Moreover, for the arbitrary selection of $\boldsymbol{a_0}, \boldsymbol{b_0} \in \boldsymbol{X}$, the sequence generated by the q-HSATM converges to fixed point of $\boldsymbol{G}$ and

$$\|\boldsymbol{w_m} - \boldsymbol{w_n}\| \leq \frac{\boldsymbol{\gamma^n}}{\mathbf{1}-\boldsymbol{\gamma}}\|\boldsymbol{w_1} - \boldsymbol{w_0}\|, \forall \boldsymbol{a}, \boldsymbol{b} \in \boldsymbol{X}. \tag{30}$$

4. THE NUMERICAL SOLUTIONS OF THE TIME-FRACTIONAL COUPLED BURGERS EQUATIONS

Let us consider the nonlinear time-fractional coupled Burgers equations (TFCBEs) **[47]**

$$\begin{cases} \dfrac{\partial^{\alpha} u}{\partial \tau^{\alpha}} + u\dfrac{\partial u}{\partial \zeta} + w\dfrac{\partial u}{\partial \mu} = \dfrac{1}{Re}\left[\dfrac{\partial^2 u}{\partial \zeta^2} + \dfrac{\partial^2 u}{\partial \mu^2}\right], \\ \dfrac{\partial^{\beta} w}{\partial \tau^{\beta}} + u\dfrac{\partial w}{\partial \zeta} + w\dfrac{\partial w}{\partial \mu} = \dfrac{1}{Re}\left[\dfrac{\partial^2 w}{\partial \zeta^2} + \dfrac{\partial^2 w}{\partial \mu^2}\right], 0 < \zeta, \mu < 1, \qquad 0 < \alpha, \beta < 1, \tau > 0. \end{cases} \tag{31}$$

with initial conditions

$$\mathrm{u}(\zeta, \mu, 0) = \frac{3}{4} - \frac{1}{4(1 + \exp((\mathrm{Re}/32)(-4\zeta + 4\mu)))}, \tag{32}$$

$$\mathrm{w}(\zeta, \mu, 0) = \frac{3}{4} + \frac{1}{4(1 + \exp((\mathrm{Re}/32)(-4\zeta + 4\mu)))}, \tag{33}$$

where, Re is Reynolds number.
Now, by applying Shehu transform to Eq. (31) and by using Eqs. (32)-(33), then it is obtained as

$$\mathrm{S}[\mathrm{u}(\zeta, \mu, \tau)] - \frac{u}{s}\mathrm{u}(\zeta, \mu, 0) + \left(\frac{u}{s}\right)^{\alpha} \mathrm{S}\left[u\frac{\partial u}{\partial \zeta} + w\frac{\partial u}{\partial \mu} - \frac{1}{Re}\left[\frac{\partial^2 u}{\partial \zeta^2} + \frac{\partial^2 u}{\partial \mu^2}\right]\right] = 0, \tag{34}$$

$$\mathrm{S}[\mathrm{w}(\zeta, \mu, \tau)] - \frac{u}{s}\mathrm{w}(\zeta, \mu, 0) + \left(\frac{u}{s}\right)^{\alpha} \mathrm{S}\left[u\frac{\partial w}{\partial \zeta} + w\frac{\partial w}{\partial \mu} - \frac{1}{Re}\left[\frac{\partial^2 w}{\partial \zeta^2} + \frac{\partial^2 w}{\partial \mu^2}\right]\right] = 0, \tag{35}$$

The nonlinear operators by using Eqs. (34)-(35) are defined as

$$\begin{aligned} &\boldsymbol{N^1}[\boldsymbol{\varphi}(\boldsymbol{\zeta}, \boldsymbol{\mu}, \boldsymbol{\tau}; \boldsymbol{q}), \boldsymbol{\psi}(\boldsymbol{\zeta}, \boldsymbol{\mu}, \boldsymbol{\tau}; \boldsymbol{q})\ ] = \boldsymbol{S}[\boldsymbol{\varphi}(\boldsymbol{\zeta}, \boldsymbol{\mu}, \boldsymbol{\tau}; \boldsymbol{q})\ ] - \frac{\boldsymbol{u}}{\boldsymbol{s}}\mathbf{u}(\boldsymbol{\zeta}, \boldsymbol{\mu}, \mathbf{0}) + \left(\frac{\boldsymbol{u}}{\boldsymbol{s}}\right)^{\boldsymbol{\alpha}} \\ &\times \left\{\boldsymbol{S}\left[\boldsymbol{\varphi}(\boldsymbol{\zeta}, \boldsymbol{\mu}, \boldsymbol{\tau}; \boldsymbol{q})\frac{\partial \boldsymbol{\varphi}(\boldsymbol{\zeta}, \boldsymbol{\mu}, \boldsymbol{\tau}; \boldsymbol{q})}{\partial \boldsymbol{\zeta}} + \boldsymbol{\psi}(\boldsymbol{\zeta}, \boldsymbol{\mu}, \boldsymbol{\tau}; \boldsymbol{q})\frac{\partial \boldsymbol{\varphi}(\boldsymbol{\zeta}, \boldsymbol{\mu}, \boldsymbol{\tau}; \boldsymbol{q})}{\partial \boldsymbol{\mu}} - \frac{\mathbf{1}}{\boldsymbol{Re}}\left[\frac{\partial^2 \boldsymbol{\varphi}(\boldsymbol{\zeta}, \boldsymbol{\mu}, \boldsymbol{\tau}; \boldsymbol{q})}{\partial \boldsymbol{\zeta}^2}\right.\right. \\ &\left.\left. + \frac{\partial^2 \boldsymbol{\varphi}(\boldsymbol{\zeta}, \boldsymbol{\mu}, \boldsymbol{\tau}; \boldsymbol{q})}{\partial \boldsymbol{\mu}^2}\right]\right\}, \end{aligned} \tag{36}$$

$$\begin{aligned} &\boldsymbol{N^2}[\boldsymbol{\varphi}(\boldsymbol{\zeta}, \boldsymbol{\mu}, \boldsymbol{\tau}; \boldsymbol{q}), \boldsymbol{\psi}(\boldsymbol{\zeta}, \boldsymbol{\mu}, \boldsymbol{\tau}; \boldsymbol{q})\ ] = \boldsymbol{S}[\boldsymbol{\psi}(\boldsymbol{\zeta}, \boldsymbol{\mu}, \boldsymbol{\tau}; \boldsymbol{q})\ ] - \frac{\boldsymbol{u}}{\boldsymbol{s}}\mathbf{w}(\boldsymbol{\zeta}, \boldsymbol{\mu}, \mathbf{0}) + \left(\frac{\boldsymbol{u}}{\boldsymbol{s}}\right)^{\boldsymbol{\alpha}} \\ &\times \left\{\boldsymbol{S}\left[\boldsymbol{\varphi}(\boldsymbol{\zeta}, \boldsymbol{\mu}, \boldsymbol{\tau}; \boldsymbol{q})\frac{\partial \boldsymbol{\psi}(\boldsymbol{\zeta}, \boldsymbol{\mu}, \boldsymbol{\tau}; \boldsymbol{q})}{\partial \boldsymbol{\zeta}} + \boldsymbol{\psi}(\boldsymbol{\zeta}, \boldsymbol{\mu}, \boldsymbol{\tau}; \boldsymbol{q})\frac{\partial \boldsymbol{\psi}(\boldsymbol{\zeta}, \boldsymbol{\mu}, \boldsymbol{\tau}; \boldsymbol{q})}{\partial \boldsymbol{\mu}} - \frac{\mathbf{1}}{\boldsymbol{Re}}\left[\frac{\partial^2 \boldsymbol{\psi}(\boldsymbol{\zeta}, \boldsymbol{\mu}, \boldsymbol{\tau}; \boldsymbol{q})}{\partial \boldsymbol{\zeta}^2}\right.\right. \\ &\left.\left. + \frac{\partial^2 \boldsymbol{\psi}(\boldsymbol{\zeta}, \boldsymbol{\mu}, \boldsymbol{\tau}; \boldsymbol{q})}{\partial \boldsymbol{\mu}^2}\right]\right\}. \end{aligned} \tag{37}$$

By applying the proposed algorithm, the $m - th$ order deformation equation is defined by

$$\mathrm{S}[u_m(\zeta, \mu, \tau) - k_m u_{m-1}(\zeta, \mu, \tau)] = h\mathcal{R}_{1,m}(\vec{u}_{m-1}), \tag{38}$$

$$\mathrm{S}[w_m(\zeta, \mu, \tau) - k_m w_{m-1}(\zeta, \mu, \tau)] = h\mathcal{R}_{2,m}(\vec{w}_{m-1}). \tag{39}$$

where

$$\boldsymbol{\mathcal{R}_{1,m}(\vec{u}_{m-1}) = S[\vec{u}_{m-1}(\zeta,\mu,\tau)\,] - \frac{u}{s}\mathbf{u}(\zeta,\mu,\mathbf{0}) + \left(\frac{u}{s}\right)^{\alpha}}$$
$$\times\left\{\boldsymbol{S}\left[\sum_{r=0}^{m-1}\boldsymbol{u_r}\frac{\partial u_{m-1-r}}{\partial\zeta} + \sum_{r=0}^{m-1}\boldsymbol{w_r}\frac{\partial u_{m-1-r}}{\partial\mu} - \frac{1}{Re}\left[\frac{\partial^2 u_{m-1}}{\partial\zeta^2} + \frac{\partial^2 u_{m-1}}{\partial\mu^2}\right]\right]\right\}, \quad (40)$$

$$\boldsymbol{\mathcal{R}_{2,m}(\vec{w}_{m-1}) = S[\vec{w}_{m-1}(\zeta,\mu,\tau)\,] - \frac{u}{s}\mathbf{w}(\zeta,\mu,\mathbf{0}) + \left(\frac{u}{s}\right)^{\alpha}}$$
$$\times\left\{\boldsymbol{S}\left[\sum_{r=0}^{m-1}\boldsymbol{u_r}\frac{\partial w_{m-1-r}}{\partial\zeta} + \sum_{r=0}^{m-1}\boldsymbol{w_r}\frac{\partial w_{m-1-r}}{\partial\mu} - \frac{1}{Re}\left[\frac{\partial^2 w_{m-1}}{\partial\zeta^2} + \frac{\partial^2 w_{m-1}}{\partial\mu^2}\right]\right]\right\}. \quad (41)$$

On applying inverse Shehu transform to Eqs. (38)-(39), then we have

$$u_m(\zeta,\mu,\tau) = k_m u_{m-1}(\zeta,\mu,\tau) + hS^{-1}\left[\mathcal{R}_{1,m}(\vec{u}_{m-1})\right], \quad (42)$$
$$w_m(\zeta,\mu,\tau) = k_m w_{m-1}(\zeta,\mu,\tau) + hS^{-1}\left[\mathcal{R}_{2,m}(\vec{w}_{m-1})\right]. \quad (43)$$

By the use of initial conditions, then it is obtained as

$$u_0(\zeta,\mu,\tau) = \frac{3}{4} - \frac{1}{4(1+\exp((\mathrm{Re}/32)(-4\zeta+4\mu)))}, \quad (44)$$
$$w_0(\zeta,\mu,\tau) = \frac{3}{4} + \frac{1}{4(1+\exp((\mathrm{Re}/32)(-4\zeta+4\mu)))}. \quad (45)$$

To find the values of $u_1(\zeta,\mu,\tau)$ and $w_1(\zeta,\mu,\tau)$, putting $m=1$ in Eqs. (42)-(43), then it is obtained as

$$u_1(\zeta,\mu,\tau) = \mathrm{hRe}\frac{\exp(-\mathrm{Re}(\zeta-\mu)/8)t^{\alpha}}{128(1+\exp(-\mathrm{Re}(\zeta-\mu)/8))^2\Gamma(\alpha+1)}, \quad (46)$$
$$w_1(\zeta,\mu,\tau) = -\mathrm{hRe}\frac{\exp(-\mathrm{Re}(\zeta-\mu)/8)t^{\beta}}{128(1+\exp(-\mathrm{Re}(\zeta-\mu)/8))^2\Gamma(\beta+1)}. \quad (47)$$

Similarly, to find values of $u_2(\zeta,\mu,\tau)$ and $w_2(\zeta,\mu,\tau)$, putting $m=2$ in Eqs. (42)-(43), then it is found as

$$u_2(\zeta,\mu,\tau) = (\mathrm{n}+\mathrm{h})\mathrm{hRe}\frac{\exp(-\mathrm{Re}(\zeta-\mu)/8)t^{\alpha}}{128(1+\exp(-\mathrm{Re}(\zeta-\mu)/8))^2\Gamma(\alpha+1)},$$
$$-\mathrm{h}^2\mathrm{Re}^2\frac{\exp(-\mathrm{Re}(\zeta-\mu)/8)}{4096(1+\exp(-\mathrm{Re}(\zeta-\mu)/8))^4\Gamma(\alpha+1)\Gamma(\beta+1)}$$
$$\times\left[\left(\frac{-\Gamma(\alpha+1)\Gamma(\beta+1)t^{2\alpha}}{\Gamma(2\alpha+1)} + \frac{\Gamma(\alpha+1)\Gamma(\beta+1)t^{\alpha+\beta}}{\Gamma(\alpha+\beta+1)}\right)\exp(-\mathrm{Re}(\zeta-\mu)/8)\right.$$
$$\left.+\frac{\Gamma(\alpha+1)\Gamma(\beta+1)(\exp(-\mathrm{Re}(\zeta-\mu)/4)-1)t^{2\alpha}}{\Gamma(2\alpha+1)}\right]. \quad (48)$$

$$w_2(\zeta,\mu,\tau) = -(\mathrm{n}+\mathrm{h})\mathrm{hRe}\frac{\exp(-\mathrm{Re}(\zeta-\mu)/8)t^{\beta}}{128(1+\exp(-\mathrm{Re}(\zeta-\mu)/8))^2\Gamma(\beta+1)},$$
$$+\mathrm{h}^2(\mathrm{Re})^2\frac{\exp(-\mathrm{Re}(\zeta-\mu)/8)}{4096(1+\exp(-\mathrm{Re}(\zeta-\mu)/8))^4\Gamma(\alpha+1)\Gamma(\beta+1)}$$

$$\times\left[\left(\frac{-\Gamma(\alpha+1)\Gamma(\beta+1)t^{2\beta}}{\Gamma(2\beta+1)}+\frac{\Gamma(\alpha+1)\Gamma(\beta+1)t^{\alpha+\beta}}{\Gamma(\alpha+\beta+1)}\right)\exp(-\mathrm{Re}(\zeta-\mu)/8)\right.$$
$$\left.+\frac{\Gamma(\alpha+1)\Gamma(\beta+1)(\exp(-\mathrm{Re}(\zeta-\mu)/4)-1)t^{2\beta}}{\Gamma(2\beta+1)}\right]. \tag{49}$$

In this way, the other terms can be obtained. Thus, the q-HSATM solution of Eq. (31) is given by

$$\mathrm{u}(\zeta,\mu,\tau)=u_0(\zeta,\mu,\tau)+\sum_{m=1}^{\infty}u_m(\zeta,\mu,\tau)\left(\frac{1}{n}\right)^m, \tag{50}$$

$$\mathrm{w}(\zeta,\mu,\tau)=w_0(\zeta,\mu,\tau)+\sum_{m=1}^{\infty}w_m(\zeta,\mu,\tau)\left(\frac{1}{n}\right)^m. \tag{51}$$

Substituting the values of $\alpha=1,\beta=1,n=1,\ h=-1$ in Eqs. (50)-(51), then the obtained results $\sum_{m=1}^{M}u_m(\zeta,\mu,\tau)\left(\frac{1}{n}\right)^m$ and $\sum_{m=1}^{M}w_m(\zeta,\mu,\tau)\left(\frac{1}{n}\right)^m$ converge to the analytical solutions $\mathrm{u}(\zeta,\mu,\tau)=\frac{3}{4}-\frac{1}{4(1+\exp((\mathrm{Re}/32)(-4\zeta+4\mu-\tau)))}$ and $\mathrm{w}(\zeta,\mu,\tau)=\frac{3}{4}+\frac{1}{4(1+\exp((\mathrm{Re}/32)(-4\zeta+4\mu-\tau)))}$ of TFCBEs when $M\to\infty$.

Figure 1 shows 3D graphs for the $\mathrm{u}(\zeta,\mu,\tau)$ solution of q-HSATM, the exact solution, and the absolute error for $\alpha=1,\ \beta=1$.

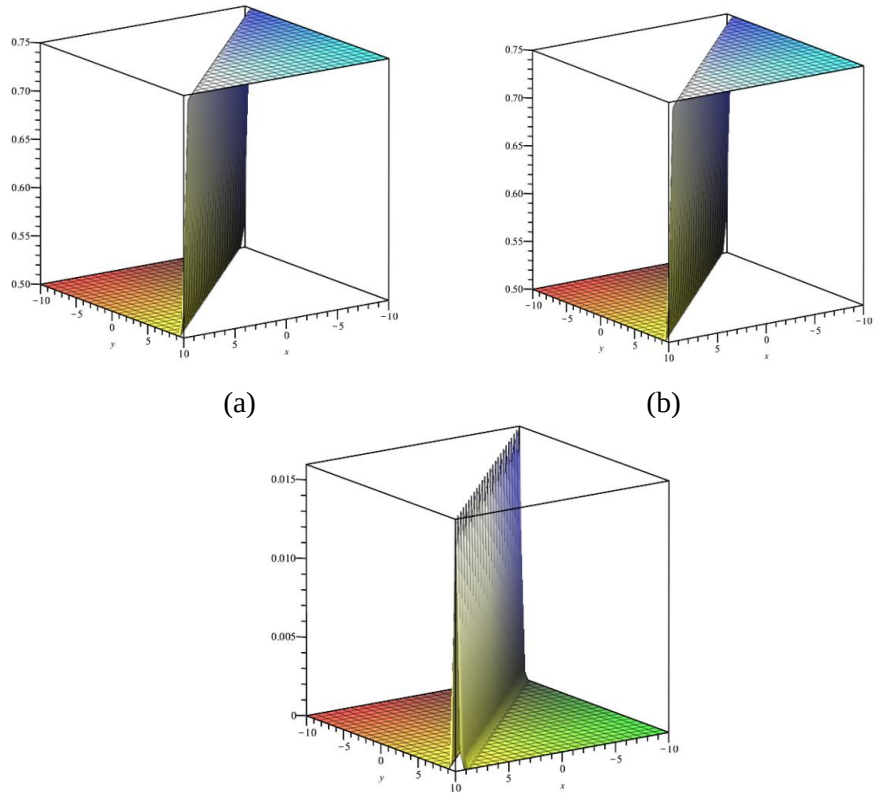

(a) (b)

(c)

Figure 1. (a) $\mathrm{u}(\zeta,\mu,\tau)$ solution of q-HSATM **(b)** Exact solution of $\mathrm{u}(\zeta,\mu,\tau)$ **(c)** Nature of absolute error=$\left|u_{exact}-u_{q-HSATM}\right|$ at $Re=100,\mathrm{h}=-1,\mathrm{n}=1,\tau=0.5,\alpha=1,\beta=1$.

Figure 2 shows 3D graphs for the $w(\zeta,\mu,\tau)$ solution of q-HSATM, the exact solution, and the absolute error for $\alpha = 1,\ \beta = 1$.

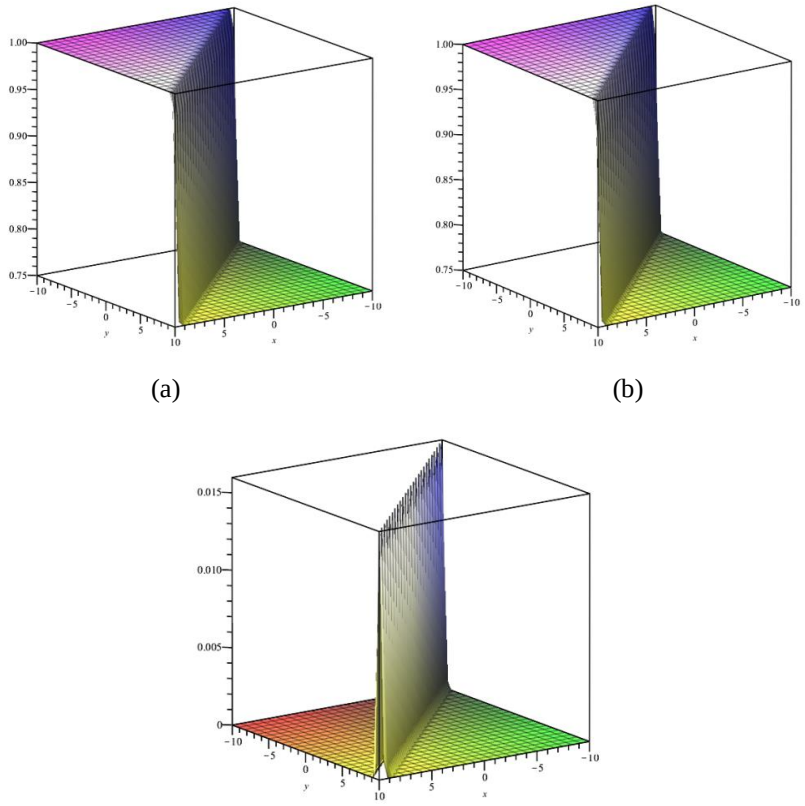

Figure 2. **(a)** $w(\zeta,\mu,\tau)$ solution of q-HSATM **(b)** Exact solution of $w(\zeta,\mu,\tau)$**(c)** Nature of absolute error=$\left|w_{exact} - w_{q-HSATM}\right|$ at $Re = 100, h = -1, n = 1, \tau = 0.5, \alpha = 1, \beta = 1$.

The 2D graphs for q-HSATM solution by varying α and β values are depicted in Figure 3.

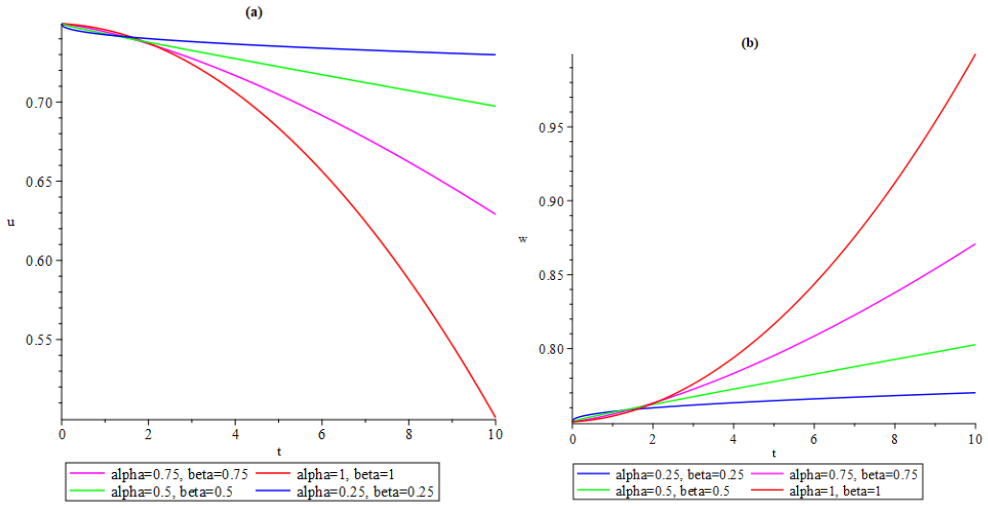

Figure 3. **(a)** $u(\zeta,\mu,\tau)$ solution of q-HSATM with respect to t when $Re = 100, x = 0.5, y = 1$ with distinct α and β. **(b)** $w(\zeta,\mu,\tau)$ solution of q-HSATM with respect to t when $Re = 100, x = 0.5, y = 1$ with distinct α and β.

q-HSATM is observed to be more efficient than FNTDM for u(ζ, μ, τ) numerical solution Table 1.

Table 1. Comparative study between FNTDM **[47]** and q-HSATM for the numierical solutions u(ζ, μ, τ) at Re $= 100,\ y = 1, \alpha = 1$ and $\beta = 1$.

ζ	τ	$\lvert u_{exact} - u_{FNTDM} \rvert$	$\lvert u_{exact} - u_{q-HSATM} \rvert$
0.1	0.1	8.4×10^{-5}	1.7×10^{-8}
	0.2	8.2×10^{-5}	1.5×10^{-7}
	0.3	7.8×10^{-5}	5.7×10^{-7}
	0.4	7.4×10^{-5}	1.4×10^{-6}
	0.5	6.9×10^{-5}	3.2×10^{-6}
0.2	0.1	9.9×10^{-4}	6.2×10^{-8}
	0.2	9.9×10^{-4}	5.4×10^{-7}
	0.3	9.7×10^{-4}	2.0×10^{-6}
	0.4	9.6×10^{-4}	5.2×10^{-6}
	0.5	9.4×10^{-4}	1.1×10^{-5}
0.3	0.1	1.1×10^{-2}	2.1×10^{-7}
	0.2	1.1×10^{-2}	1.8×10^{-6}
	0.3	1.1×10^{-2}	6.9×10^{-6}
	0.4	1.1×10^{-2}	1.8×10^{-5}
	0.5	1.1×10^{-2}	3.9×10^{-5}
0.4	0.1	1.3×10^{-1}	7.5×10^{-7}
	0.2	1.3×10^{-1}	6.5×10^{-6}
	0.3	1.3×10^{-1}	2.4×10^{-5}
	0.4	1.3×10^{-1}	6.3×10^{-5}
	0.5	1.3×10^{-1}	1.3×10^{-4}
0.5	0.1	1.5×10^{0}	2.6×10^{-6}
	0.2	1.5×10^{0}	2.2×10^{-5}
	0.3	1.5×10^{0}	8.3×10^{-5}
	0.4	1.5×10^{0}	2.1×10^{-4}
	0.5	1.5×10^{0}	4.6×10^{-4}

In Table 2, q-HSATM is observed to be more efficient than FNTDM for w(ζ, μ, τ) numerical solution.

Table 2. Comparative study between FNTDM **[47]** and q-HSATM for the numerical solutions w(ζ, μ, τ) at Re $= 100,\ y = 1, \alpha = 1$ and $\beta = 1$.

ζ	τ	$\lvert w_{exact} - w_{FNTDM} \rvert$	$\lvert w_{exact} - w_{q-HSATM} \rvert$
0.1	0.1	3.4×10^{-5}	1.7×10^{-8}
	0.2	1.3×10^{-5}	1.5×10^{-7}
	0.3	4.2×10^{-6}	5.7×10^{-7}
	0.4	2.8×10^{-6}	1.4×10^{-6}
	0.5	9.9×10^{-6}	3.2×10^{-6}
0.2	0.1	2.9×10^{-5}	6.2×10^{-8}
	0.2	1.5×10^{-6}	5.4×10^{-7}
	0.3	1.5×10^{-5}	2.0×10^{-6}
	0.4	3.3×10^{-5}	5.2×10^{-6}
	0.5	5.3×10^{-5}	1.1×10^{-5}
0.3	0.1	9.1×10^{-6}	2.1×10^{-7}
	0.2	4.1×10^{-5}	1.8×10^{-6}
	0.3	8.6×10^{-5}	6.9×10^{-6}
	0.4	1.3×10^{-4}	1.8×10^{-5}
	0.5	2.0×10^{-4}	3.9×10^{-5}
0.4	0.1	6.0×10^{-5}	7.5×10^{-7}
	0.2	1.8×10^{-4}	6.5×10^{-6}
	0.3	3.3×10^{-4}	2.4×10^{-5}
	0.4	5.0×10^{-4}	6.3×10^{-5}
	0.5	7.2×10^{-4}	1.3×10^{-4}
0.5	0.1	3.0×10^{-4}	2.6×10^{-6}
	0.2	7.0×10^{-4}	2.2×10^{-5}
	0.3	1.1×10^{-3}	8.3×10^{-5}
	0.4	1.7×10^{-3}	2.1×10^{-4}
	0.5	2.5×10^{-3}	4.6×10^{-4}

5. CONCLUSION

q-HSATM is used to analyze the coupled Burgers equations in this paper. In addition, MAPLE software was used to obtain the graphs of the numerical solutions of these equations for the various alpha and beta values. For coupled Burgers equations, it is observed that the general structure of surface graphs plotted in Maple software differs. Coupled Burgers equations for which numerical solutions have been quickly and successfully obtained. Therefore, it may be extrapolated that q-HSATM is overly effective and robust for obtaining numerical solutions for various fractional nonlinear partial differential equations.

ACKNOWLEDGEMENTS

We would like to thank the referees for their contributions.

CONFLICT OF INTEREST

The authors stated that there are no conflicts of interest regarding the publication of this article.

AUTHORSHIP CONTRIBUTIONS

Autors' contributions are equal.

REFERENCES

[1] Hilfer R. Application of Fractional Calculus in Physics, Singapore, World Scientific Publishing Company, 2000.

[2] Kilbas A, Srivastava, H, Trujillo J. Theory and Applications of Fractional Differential Equations, Amsterdam, Elsevier, 2006.

[3] Miller KS, Ross B. An Introduction to the Fractional Calculus and Fractional Differential Equations, New York, Wiley, 1993.

[4] Oldham KB, Spanier J. The Fractional Calculus, New York, Academic Press, 1974.

[5] Podlubny I. Fractional Differential Equations, New York, Academic Press, New York, 1999.

[6] Samko SG, Kilbas AA, Marichev OI. Fractional Integrals and Derivatives Theory and Applications, New York, Gordon and Beach, 1993.

[7] Metzler R, Nonnenmacher TF. Space-and time-fractional diffusion and wave equations, fractional Fokker-Planck equations, and physical motivation. Chemical Physics, 2002; 284 (1-2), 67-90.

[8] Metzler R, Klafter J. The random walk's guide to anomalous diffusion: a fractional dynamics approach. Physics reports, 2000; 339 (1), 1-77.

[9] Morgado ML, Rebelo M. Numerical approximation of distributed order reaction–diffusion equations. Journal of Computational and Applied Mathematics, 2015; 275, 216-227.

[10] Abu-Gdairi R, Al-Smadi M, Gumah G. An expansion iterative technique for handling fractional differential equations using fractional power series scheme. Journal of Mathematics and Statistics, 2015; 11(2), 29–38.

[11] Baleanu D, Golmankhaneh AK, Baleanu MC. Fractional electromagnetic equations using fractional forms. International Journal of Theoretical Physics, 2009; 48(11), 3114–3123.

[12] Baleanu D, Jajarmi A, Hajipour M. On the nonlinear dynamical systems within the generalized fractional derivatives with Mittag–Leffler kernel. Nonlinear Dynamics, 2018(1), 1–18.

[13] Baleanu D, Asad JH, Jajarmi A. New aspects of the motion of a particle in a circular cavity. Proceedings of the Romanian Academy Series A, 2018; 19(2), 143–149.

[14] Baleanu D, Jajarmi A, Bonyah E, Hajipour M. New aspects of poor nutrition in the life cycle within the fractional calculus. Advances in Difference Equations, 2018; 2018(1), 1-14.

[15] Jajarmi A, Baleanu D. Suboptimal control of fractional-order dynamic systems with delay argument. Journal of Vibration and Control, 2018; 24(12), 2430-2446.

[16] Jajarmi A, Baleanu D. A new fractional analysis on the interaction of HIV with CD4+ T-cells. Chaos, Solitons & Fractals, 2018; 113, 221-229.

[17] He JH. Addendum: new interpretation of homotopy perturbation method. International Journal of Modern Physics B, 2006; 20(18), 2561-2568.

[18] Laskin, N. Fractional quantum mechanics. Physical Review E, 2000; 62(3), 3135-3145.

[19] Mainardi F. Fractional Calculus and Waves in Linear Viscoelasticity, London, Imperial College Press, 2010.

[20] Wazwaz AM. A reliable modification of Adomian decomposition method. Applied Mathematics and Computation, 1999; 102(1), 77-86.

[21] He JH. Homotopy perturbation method: a new nonlinear analytical technique. Applied Mathematics and Computation, 2003; 135(1), 73-79.

[22] He JH. Homotopy perturbation method for solving boundary value problems. Physics Letters, 2006; 350(1-2), 87-88.

[23] He JH. Addendum: new interpretation of homotopy perturbation method. International Journal of Modern Physics B, 2006; 20(18), 2561-2568.

[24] Alkan A. Improving homotopy analysis method with an optimal parameter for time-fractional Burgers equation, Karamanoğlu Mehmetbey Üniversitesi Mühendislik ve Doğa Bilimleri Dergisi, 2022; 4(2), 117-134.

[25] Turkyilmazoglu M. Convergence accelerating in the homotopy analysis method: a new approach. Advances in Applied Mathematics and Mechanics, 2018; 10(4).

[26] Yüzbaşı Ş. A numerical approximation for Volterra's population growth model with fractional order. Applied Mathematical Modelling, 2013; 37(5), 3216-3227.

[27] Yüzbaşı Ş. Numerical solutions of fractional Riccati type differential equations by means of the Bernstein polynomials. Applied Mathematics and Computation, 2013; 219(11), 6328-6343.

[28] Yüzbaşı Ş. Numerical solutions of hyperbolic telegraph equation by using the Bessel functions of first kind and residual correction. Applied Mathematics and Computation, 2016; 287, 83-93.

[29] Yüzbaşı Ş. A collocation method for numerical solutions of fractional-order logistic population model. International Journal of Biomathematics, 2016; 9(2), 1650031.

[30] Yüzbaşı Ş. A numerical method for solving second-order linear partial differential equations under Dirichlet, Neumann and Robin boundary conditions. International Journal of Computational Methods, 2017; 14(2), 1750015.

[31] Yüzbaşı Ş. A collocation approach for solving two-dimensional second-order linear hyperbolic equations. Applied Mathematics and Computation, 2018; 338, 101-114.

[32] Merdan M, Anaç H, Kesemen T. The new Sumudu transform iterative method for studying the random component time-fractional Klein-Gordon equation. Sigma, 2019; 10(3), 343-354.

[33] Wang K, Liu S. A new Sumudu transform iterative method for time-fractional Cauchy reaction-diffusion equation. Springer Plus, 2016; 5(1), 865.

[34] Anaç H, Merdan M, Bekiryazıcı Z, Kesemen T. Bazı Rastgele Kısmi Diferansiyel Denklemlerin Diferansiyel Dönüşüm Metodu ve Laplace-Padé Metodu Kullanarak Çözümü. Gümüşhane Üniversitesi Fen Bilimleri Enstitüsü Dergisi, 2019; 9(1), 108-118.

[35] Ayaz F. Solutions of the system of differential equations by differential transform method. Applied Mathematics and Computation, 2004; 147(2), 547-567.

[36] Kangalgil F, Ayaz F. Solitary wave solutions for the KdV and mKdV equations by differential transform method. Chaos, Solitons & Fractals, 2009; 41(1), 464-472.

[37] Merdan M. A new applicaiton of modified differential transformation method for modeling the pollution of a system of lakes. Selçuk Journal of Applied Mathematics, 2010; 11(2), 27-40.

[38] Zhou JK. Differential Transform and Its Applications for Electrical Circuits. Wuhan, Huazhong University Press, 1986.

[39] Maitama S, Zhao W. New integral transform: Shehu transform a generalization of Sumudu and Laplace transform for solving differential equations. arXiv preprint arXiv:1904.11370. (2019).

[40] Akinyemi L, Iyiola OS. Exact and approximate solutions of time-fractional models arising from physics via Shehu transform. Mathematical Methods in the Applied Sciences,2020; 43(12), 7442-7464.

[41] Alfaqeih S, Misirli E. On double Shehu transform and its properties with applications. International Journal of Analysis and Applications, 2020; 18(3), 381-395.

[42] Maitama S, Zhao W. Homotopy analysis Shehu transform method for solving fuzzy differential equations of fractional and integer order derivatives. Computational and Applied Mathematics, 2021; 40(3), 1-30.

[43] Kanth AR, Aruna K, Raghavendar K, Rezazadeh H, İnç M. Numerical solutions of nonlinear time fractional Klein-Gordon equation via natural transform decomposition method and iterative Shehu transform method. Journal of Ocean Engineering and Science, https://doi.org/10.1016/j.joes.2021.12.002. (2021).

[44] Shah R, Saad Alshehry A, Weera W. A semi-analytical method to investigate fractional-order gas dynamics equations by Shehu transform. Symmetry, 2022; 14(7), 1458.

[45] Abujarad ES, Jarad F, Abujarad MH, Baleanu D. Application of q-Shehu transform on q-fractional kinetic equation involving the generalizd hyper-Bessel function. Fractals, 2022; 30(05), 2240179.

[46] Sinha AK, Panda S. Shehu Transform in Quantum Calculus and Its Applications. International Journal of Applied and Computational Mathematics, 2022; 8(1), 1-19.

[47] Prakasha DG, Veeresha P, Rawashdeh MS. Numerical solution for (2+ 1)-dimensional time-fractional coupled Burger equations using fractional natural decomposition method. Mathematical Methods in the Applied Sciences, 2019; 42(10), 3409-3427.

[48] Cole JD, On a quasi-linear parabolic equation occurring in aerodynamics. Quarterly of Applied Mathematics, 1951; 9, 225–236.

[49] Aksan EN. Quadratic B-spline fifinite element method for numerical solution of the Burgers equation. Appl. Math. Comput., 2006; 174, 884–896.

[50] Kutluay S, Esen A. A lumped Galerkin method for solving the Burgers equation. Int. J. Comput. Math., 2004; 81, 1433–1444.

[51] Abbasbandy S, Darvishi MT. A numerical solution of Burgers equation by modifified Adomian method. Appl. Math. Comput., 2005; 163, 1265–1272.

[52] Jin-Ming Z, Yao-Ming Z, Abd AL-Hussein WR, Mahmood A, Shamran SNK. Exact solutions of the two-dimensional Burgers equation. J. Phys. A Math. Gen., 1999; 32, 6897–6900.

[53] Bateman H. Some recent researches on the motion of fluids. Monthly Weather Review, 1915; 43, 163–170.

[54] Hopf E. The partial differential equation ut + uux = uxx. Commun. Pure Appl. Math., 1950; 3, 201–230.

[55] Benton ER, Platzman GW. A table of solutions of the one-dimensional Burgers equation. Q. Appl. Math., 1972; 30, 195–212.

[56] Karpman VI. Non-Linear Waves in Dispersive Media: International Series of Monographs in Natural Philosophy, Amsterdam, The Netherlands, Elsevier, 2016.

[57] Aljahdaly NH, Agarwal RP, Shah R, Botmart T. Analysis of the time fractional-order coupled burgers equations with non-singular kernel operators. Mathematics, 2021; 9(18), 2326.

[58] Anaç H, Merdan M, Kesemen T. Solving for the random component time-fractional partial differential equations with the new Sumudu transform iterative method. SN Applied Sciences, 2020; 2(6), 1-11.

[59] Yüzbaşı Ş. Fractional Bell collocation method for solving linear fractional integro-differential equations. Mathematical Sciences, 2022; 1-12.

[60] Kumar D, Singh J, Baleanu D. A new analysis for fractional model of regularized long-wave equation arising in ion acoustic plasma waves. Mathematical Methods in the Applied Sciences, 2017; 40(15), 5642-5653.

[61] Magreñán ÁA. A new tool to study real dynamics: The convergence plane. Applied Mathematics and Computation, 2014; 248, 215-224.

ESKİŞEHİR TECHNICAL UNIVERSITY JOURNAL OF SCIENCE AND TECHNOLOGY
A- APPLIED SCIENCES AND ENGINEERING

2023, 24(3), pp. 192-206, DOI:10.18038/estubtda.1335496

RESEARCH ARTICLE

THE USE OF COX REGRESSION MODEL IN THE SURVIVAL ANALYSIS FOR LEUKEMIA PATIENTS IN THE REPUBLIC OF YEMEN.

Elias AL-SAMAI [1], **Sevil ŞENTÜRK** [2]

[1] Department of Statistics, Faculty of Administrative Sciences, Taiz University, Taiz, Yemen
[2] Department of Statistics, Faculty of Science, Eskisehir Technical University, Eskisehir, Türkiye

ABSTRACT

This study aims at analyzing and studying the theoretical and practical importance of the (Cox) regression model in the analysis of survival as well as measuring the most important factors affecting the survival time for patients with leukemia. Moreover, it aims at reaching the expected survival time for patients and creating a life table for patients by using (Cox) regression model. To achieve these goals, real data were taken for (1168) patients with leukemia in the Republic of Yemen in the period from January 2017 to February 2022. The dependent variable, which is the patient's condition at the end of the period, was determined in addition to the patient's survival time and eight independent variables were identified. The effect of these variables on the survival time of patients with leukemia was investigated using the SPSS program. The study concluded several results, the most prominent of them are the following: There are no differences in the incidence rate between males and females and the most age group affected by this disease is (40 years and over). Furthermore, it was found that acute lymphoblastic leukemia (ALL) is the most prevalent type among the other types and there is a difference in the risk of death among those who take intravenous chemotherapy and those patients who take oral chemotherapy. Other significant result was found that there is a higher risk of death for non-regular patients in receiving treatment compared to regular patients in receiving treatment. It was found that the most influencing variables on the survival time of patients are (age, marital status, type of disease, the governorate in which the patient lives, regularity in receiving treatment and type of chemotherapy). Through the life table, it is noticed that the greatest risk in the survival time is in the thirty-sixth month, which is the largest among all other periods, as it reached (0.10). Additionally, the median survival time was reached (35.06) months. Finally, the study found that there are differences in the incidence according to the type of disease in terms of the risk of death as acute lymphoblastic leukemia (ALL) is the most prevalent disease among all diseases and the largest percentage of deaths was among those with chronic myeloid leukemia (CML).

Keywords: Cox Regression, Survival Analysis, Censored, Event

1. INTRODUCTION

Survival analysis is considered as the study of the time of a specific variable until the occurrence of the event as it deals with the time preceding the occurrence of a specific event and one of the most applied examples in this field is the study of the time preceding death. The survival analysis is applied in many different fields such as medicine, engineering, economics, social sciences and others fields where the element of time until the occurrence of a specific event is the main factor for the phenomenon under study.[1,2] In other words, survival analysis is the phrase that is used to describe the analysis of data in the form of times from the original time until the occurrence of a certain event or a certain end point. From the foregoing, it can be said that survival analysis is a set of statistical procedures for analyzing data when the dependent variable (the variable of interest) represents the time until the occurrence of the event. This time may be days, weeks, months or years from the beginning of the item until the

*Corresponding Author:elias.aqlan@taiz.edu.ye
Received:01.07.2023 Published. 22.09.2023

occurrence of the event. The event occurs only once for each item of the study. This event may be death, relapse of the patient...etc. [3,4]

Due to the importance of the topic of survival time and its impact on multiple factors, the urgent need has emerged to develop methods and statistical means to increase accuracy, comprehensive and broad knowledge of the factors affecting the survival of the injured person whether alive or dead within the study period. Among these methods are regression models which are not in their traditional form but rather in a developed form. Such developed form should fit the case of the dependent variable which is bi-response.

One of these models and the most widely used is the (cox) regression model proposed by the English scientist (Cox Dived) in 1972 AD. It is considered one of the appropriate models for binary data through which the survival time and the factors affecting the survival time of the injured person are studied. This model aims at knowing the risk factors that significantly affect the risk function during the duration of time. Furthermore, survival analysis of the Cox regression model involves examining the time from patient admission to the study period until the onset of the event (death) or Censored [5,6].

The problem of the study emerged from the fact that leukemia is one of the most common diseases that leads to the death of thousands of people .Thus, this study focuses on studying and identifying the factors affecting the survival times of leukemia patients in the Republic of Yemen.

In order to identify these factors, Cox regression model was applied as survival analysis is necessary when studying systems in which the dependent variable is the time until a certain event occurs and survival analysis is widely applied in medical and biological studies. Applying such models to different diseases helps in identifying the conditions and characteristics that lead to increasing or decreasing the probability of survival and the factors affecting it. Consequently, the problem of the current study seeks as well at identifying the most important variables affecting the survival time through the Cox regression model and the significant of this study lies on shedding light on survival analysis models especially the (Cox) regression model which makes this study a starting point for other studies.

Mainly, the aims of the current study is based on two main aims which they are measuring the most important influencing factors (risk factors) on the survival time of leukemia patients in the Republic of Yemen by using the (Cox) model and estimating the survival and hazard function of this model as well as forming life table.Consequently the current study identifies the most important factors affecting the survival time of leukemia patients in the Republic of Yemen based on real data form the period January 2017 to the period February 2022 for 1168 patients diagnosed with leukemia.

The hypothesis of the study (H_0) is based on the assumption that there is no significant effect of the variables (sex, age, blood type, marital status, type of disease, the province in which the patient lives, regularity in receiving treatment and type of chemotherapy) on the probability of survival at a significant level of 5%.

2. LITERATURE REVIEW

Okal 2010 studied the survival of breast cancer patients in the Gaza Strip as the study period spanned the period between (2000-2005) ,meanwhile the sample size was 103 women. The Cox model was used by applying (Kaplan-Meier) method to estimate the survival function as the study variables were (date of birth, marital status, address, smoking, date of injury registration, date of end of follow-up, place of appearance of infection, condition, breast containing the primary tissue tumor and treatment). The study concluded that the treatment variables and age are the two influencing variables in the survival time and the rest of the variables had no effect on the survival time.[7]

Meanwhile, the study of S. M. M. Kamal, 2011was based on data of "Social and Economic Determinants of Age at First Marriage among Tribal Women in Bangladesh". This data were collected through a field survey conducted in 2006 in Bangladesh. The study was applied to a sample of 792 currently married women born before 1986. Cox's model was used to study the determinants of age at first marriage for women. The study concluded that women ,who are working in formal jobs, have an impact on women's age at first marriage. The study also indicated that women with higher education are more likely to delay their marriage. The study showed that the place of residence and the educational status of the father have a significant impact on the timing of marriage for women as the study showed that women who were born in rural areas are more likely to marry early. Moreover, women whose fathers are illiterate are more likely to marry early compared to women whose fathers are educated as parents' focus on increasing the educational level of their children. Furthermore, the study indicated that the survival status of the fathers as well as the economic status of the fathers had an impact on the age of the woman at the first marriage. Additionally, the study showed that women whose dowry is less are more likely to marry early. The study indicated also that the order of birth among the sisters has an impact on the woman's age at the first marriage as the sisters take turns in the marriage contract.[8]

Whether, the study Of Burcu Küley Ağir, 2017 aimed at examining survival analysis methods and their application in the field of livestock. In this study, Kaplan-Meier (K-M) and Cox regression methods were applied and the data of two different samples were used in the field of livestock. The first sample is the death records of raising chickens from two different poultry houses and the second sample is the death records of two groups of mice (mice with and without treatment).

In the sample fattening chicken, the data of the rearing period of 5344 chickens were used. The follow-up time for the chickens in the two barns was determined in weeks and both of them were followed up for a period of 23 weeks.

The number of chickens in coop A was 2224 while in coop B there were 3120 chickens. 108 chickens from the first coop experienced the event (death) while 88 chickens from the second coop experienced the event (death). The results showed that there was a significant difference between groups A and B at a significant level (0.01) and the risk of chicken death from the second coop B was 1.74 times higher than that of the first coop A.

With regard to the second sample (mice), it was found that there was a significant effect attributed to the variables of sex and treatment condition and it was found that the time for tumor development in male and female mice was 103,525 and 96,202 weekly respectively. According to the treatment condition variable, the time for tumor development was 100,380 and 98,550 weekly respectively for the control and treatment groups. Finally, it was found that the treatment group had a risk of tumor development 2.193 times higher than the group (without treatment), in addition to that the male mice group had a tumor risk 0.047 times lower than that of female mice [9].

Moreover, S. Selim and S. Sülükçüler's 2023 study aimed at making a comparative analysis of the factors that affect the duration of smoking for individuals in Turkey. The data of health surveys in Turkey for the years 2012 and 2019 were used. The study was conducted on 5932 individuals in 2012 and 6833 individuals in 2019. The study variables were divided into variables (demographic, social, economic, chronic diseases and other variables in four basic categories). The study concluded that the demographic and socio-economic variables, chronic diseases and the reason for starting smoking have a significant effect on the duration of smoking. It was also found that women smoke more than men. In addition, an increase in the level of education and income contribute to an increase in the duration of smoking as well.[10]

Furthermore, Study of Çilengiroğlu Ö. 2023 aimed at finding out the factors that affect months unemployment time for students of the Statistics Department at Eylül University Dokuz 2014-2019 until they can find their first job immediately after graduation using survival analysis methods.

The time that a student takes to find his or her first job after graduation was defined as Event while the time a student takes to find a job as Censored. The results of analyzing the study data by using Kaplan-Meier and Cox regression showed that the variables (gender", higher education after graduation, satisfaction with life, training status and knowledge of computer programs and programming languages are statistically significant for the period between graduation and finding a job. The results also showed that choosing the appropriate place for training is crucial as through appropriate training graduates can find a job faster than expected. It was also found that the average survival of female graduates without work until obtaining the first opportunity reached 6 months while for male students reached 12 months [11] .

3. SURVIVAL ANALYSIS

Survival analysis is defined as a branch of statistics that includes a set of statistical techniques for analyzing data in which the variable of interest is the survival time until the event occurs and time can refer to the age of the individual when the event occurs while the event means the transition from one state to another .In the survival analysis, the event here is death, the occurrence of a certain disease or any particular experience of interest that may happen to the individual,.

As the name of survival analysis is the most widely used and recognized and it relates to the analysis of data that has three main characteristics namely:[12,13]

1. The dependent variable is the residence time until a specific event occurs.
2. The presence of control data.
3. The explanatory variables that affect the survival time and needed to be identified .

The analysis of survival functions includes time modeling for example, the study of the condition of the patient since the diagnosis of injury until the occurrence of the event (the event represents death in the literature of survival analysis in medical experiments) or monitoring (which includes recovery, withdrawal from the hospital without knowing his health condition or death due to a cause other than the reason for the study .Therefore, survival analysis is the only statistical method that deals with controlled and uncontrolled data. [14,15]

- **Survival Data:**

It is an expression used to describe data that measures the time until the event and the resulting variable, which is known as the survival time. This variable is always a positive real variable.

It can be defined as "data that measure the survival time of a group of patients with a specific disease while they are being studied until death or their loss from follow-up due to withdrawal or the end of the study period.

- **The Event**

The concept of the event differs according to the study. In medical studies and research, the event means death from a specific cause (the cause of the study) such as cancer for example. The event can be the emergence of disease, the development of disease, or the relapse of the patient. In industrial applications, the event may be the failure of the unit. In economics, an event may mean getting a job and in demography, it may mean marriage.

- **Censored Data**

The subject of Censored data is one of the topics that have applied importance in the medical and industrial fields and what distinguishes the studies of survival functions or reliability functions from other statistical studies is the phenomenon of monitoring (Censoring) in which part of the information is missing which means that there is partial information about the random variable.

It means units put to the test and the test ends when a certain number of failed units or at a predetermined time. Censoring data often appear in the study of survival especially in medical experiments when the information available about the survival time of the patient under study is incomplete for several reasons, namely:

- The probability that the person does not experience the event before the study ends.
- The possibility that the person will lose himself during the study period.
- The possibility that the person may withdraw from the study because of death (if death is not the event) or for a reason other than the reason for the study.

4. COX REGRESSION MODEL

In the seventies of the last century, various methods and techniques were used to treat the problem of regression in which the dependent variable is subject to Censoring. Some of these methods depend on assumptions about the distribution of survival times while others do not depend on assumptions about the distribution of survival times. One way in which there are no assumptions about the distribution of survival times is the Cox regression model in which it is based on the proportional hazards model .

In 1972, the English scientist (David Cox) estimated the relative risk model or what is named by cox regression model. This model determines the relationship between the explanatory (independent) variables available to the individual studied and the time of survival for them. The cox model is considered the most used model in the analysis of survival data especially when it is used in the case of monitoring data (Censored Survival Time). It aims at knowing the risk factors that contribute significantly to the risk function during the period of time until the emergence of the critical event. In 1975 the English scientist (David Cox) proposed a method to estimate the parameters of the model that he proposed in the year 1972 and he called it the partial possibility function.[16,17]

The model is defined as a statistical method for interpreting the relationship between the patient's survival time and a set of explanatory variables (risk variables) affecting the patient's survival time. The purpose of this model is to explore the effects of a number of variables on the patient's survival. The risk factors for the Cox model are similar to the independent variables in the regular regression models except that they appear in a non-linear exponential form.[18,19]

This model does not assume a specific distribution of survival times rather it assumes that the effect of the various variables is constant over time. It is also called the semi-parametric model because it includes a parametric part. The parametric part is the exponential function of the explanatory variables and a non-parametric part is the baseline hazard function and the model is one of the most important and most common models in survival analysis models as this model is used in cases where the time variable that precedes the occurrence of a particular event is of importance in analyzing the phenomenon in question.

The proposed Cox regression model:[20]

$$\boldsymbol{h(t/x) = h_0(t)\, exp \sum_{i=1}^{p} \beta_i x_i} \qquad (1)$$

where is

$\boldsymbol{h(t/x)}$ = represents the conditional hazard function of the model

It is clear from this equation (1) that the conditional risk for a specific individual at time t results from two factors:

$h_0(t)$ **:** The baseline hazard function, which depends on time, expresses the risk function when the independent variables are equal to zero ,unknown, always positive and represents the non-parametric part of the model.

$exp\sum_{i=1}^{p}\beta_i x_i$: It is the relative risk that does not depend on time in which the effect of the independent variables by increasing or decreasing the risk is constant and does not change for the change of time T.

5. DATA ANALYSIS

This section includes the practical application of the cox regression model, the analysis of the most important factors affecting survival times, the clarification of the effect of each variable on the survival time and the preparation of the life schedule. The study data were obtained from the National Cancer Foundation and the National Cancer Control Center in the Republic of Yemen for 1168 patients for the period from January 2017 to February 2022. The most important variables studied were:

- The dependent variable (Status) is the state at the end of the period for the patient which is a descriptive binary variable and indicates the patient's condition at the end of the period.
- **T**: the time variable which is the survival time of the injured person until death or observation and it was calculated on the basis of months.

Eight risk factors have been identified which can be summarized as follows:

1. Patient's gender: male or female.
2. The patient's age was divided into three categories: less than 18 years, from 18 to less than 40 years and from 40 years and over.
3. The patient's blood type: O-, AB+, A+ or O+
4. The patient's marital status: child, single, married, divorced or widowed.
5. The governorate in which the injured person lives and it has been divided into eight categories:

Taiz, Ibb, Aden, Lahj, Abyan, Al-Dhalea, Al-Hodeidah, and others

6. The type of disease which consists of four types:

Acute lymphoblastic leukemia (ALL) and acute myeloid leukemia (AML).
Chronic myeloid leukemia (CML) and chronic lymphocytic leukemia (CLL).

7. The type of chemical treatment used and it was divided into two types:

Intravenous chemotherapy and oral chemotherapy

8. Regularity in receiving treatment has been divided into:

Regular and irregular

Relative Risk Hypothesis Test:

The first step in estimating the cox model is to test the relative risk hypothesis which assumes that the risk rate is constant from one person to another over time within the study.[12]
The relative risk hypothesis is tested in two ways:

1- Drawing Method:

The hypothesis of relative risk is tested by drawing using the (Kaplan-Meier) method where one of the variables is divided into two parts and a curve drawing .Here the variable of the type of chemotherapy was divided into two parts and then a survival curve was drawn for each type as it appears that the two curves are parallel and the difference between them is constant over time. This indicates that the risk rates have a similar behavior for the two sections over the survival time of the infected person and it is noted that the hypothesis of relativity has been achieved as shown in Figure (1).

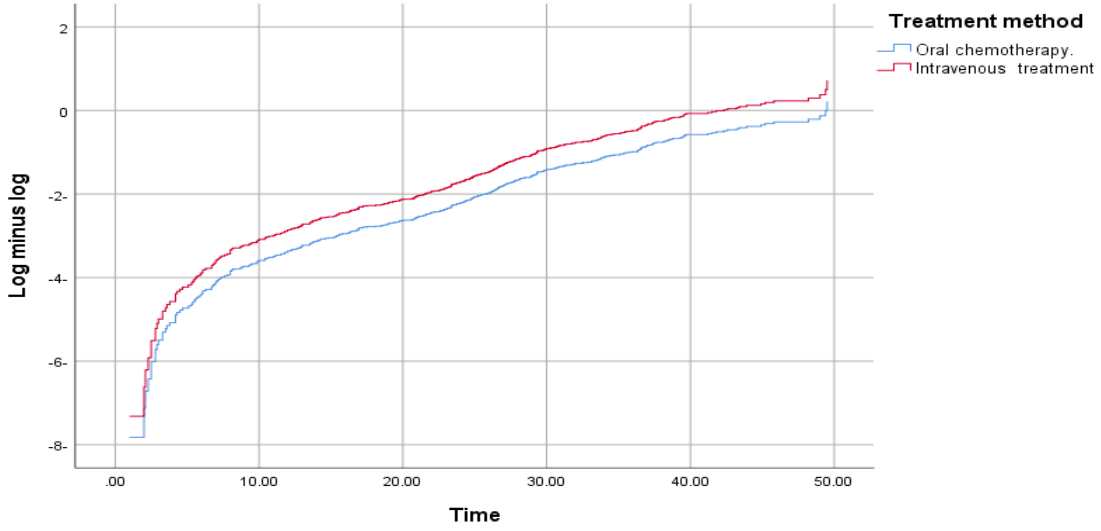

Figure 1. The Graphic Method of Proportional Hazard Hypothesis Test

2- Numerical Met

The imposition of relative risk is confirmed by the numerical method as well by testing (Schoenfeld residuals) errors and according to the null hypothesis which states that the correlation between Schoenfeld errors and survival times is equal to zero as the rejection of this hypothesis means that the relative risk condition is not fulfilled:

$$\boldsymbol{H\_0: \delta\_1 = \delta\_2 = \delta\_3 = \delta\_4 = \delta\_5 = \delta\_6 = \delta\_7 = \delta\_8 = 0}$$

Table 1. Results of the Schoenfeld Residuals Test to assume Relative Risk

Variables	Chi-square	Df	(Sig.)
Blood type	0.829	1	0.362
Sex	0.022	1	0.882
Marital status	0.593	1	0.441
Region of Living	0.142	1	0.706
Disease type	0.193	1	0.660
Treatment method	0.000	1	0.991
Regularity in receiving treatment	3,630	1	0.057
The age	0.612	1	0.434
Total model	5.209	8	0.735

Through Table (1), it is noted that the calculated value for the overall model that contains 8 variables is (5.209) at (8) degrees of freedom which is less than the tabular value (15.51). This means that it is not significant. Therefore the null hypothesis that states that all correlation coefficients between Schofield errors and survival times are equal to zero is accepted .This indicates that all variables together fulfill the hypothesis of relative risk and the same case for each variable separately. It is found that the value at one degree of freedom for each variable was less than the tabular value of (3.84) and the level of significance for all variables is mor than (0.05). This means that the correlation between Schofield errors and survival times for each variable separately is equal to zero, thus it is identical result to the graph method.

- **Parameter Estimation of Cox Regression Model:**

After realizing the hypothesis of relative risk and estimating the basic functions, the parameters of the cox regression model are estimated by the parametric side of the model using the Partial Likelihood method. It is assumed that the risk function for patients with leukemia is related to the effect of (8) of

the variables (sex, age , blood type, marital status, type of disease, the province in which the patient lives, regularity in receiving treatment and type of chemotherapy) on the survival time. Thus, the parameters were estimated using the Partial Likelihood method and Table (2) presents the results of estimating the parameters variables for the (cox) regression model as follows:

Table2. Cox Regression Model Parameters Estimation Results

Variables	B	Wald	SE	df	(Sig.)
Blood Type	0.051	0.401	0.081	1	0.527
Sex	0.016	0.022	0.106	1	0.882
Marital status	0.173	4.115	0.085	1	0.042
Region of Living	0.102	8.363	0.035	1	0.004
The type of disease	0.193	9.404	0.063	1	0.002
Type of treatment	0.453	7.859	0.162	1	0.005
Regularity in receiving treatment	1.127	106.600	0.109	1	0.005
The age	-0.216	4.599	0.101	1	0.032

From table (2), it is noted that the value of significance for the blood type and gender variables amounted respectively (0.527) and (0.882) which means that the coefficients estimated for the two variables are not significant at the level of Significant (5%). Therefore, the null hypothesis, which states that the effect of the two coefficient is zero, is accepted.

Moreover, the value of significance for the (marital status, region of living , the type of disease, type of treatment, regularity in receiving treatment and the age) variables amounted respectively (.042,0.004,0.002, 0.005, 0.005, .032) which means that the coefficients estimated for the variables are significant at the level of significance (5%). Therefore, the alternative hypothesis, that states the coefficients are not equal to zero, is accepted.

- **Testing the Significance of the Variables included in the Model:**

After estimating the parameters of the independent variables of the model, it must be known that the variables which are significant must remain in the model and which are non-significant must be deleted from the model by stepwise deletion of the overall model (Stepwise Backward). The least significant variable is deleted in the form of steps until the significant variables affecting the survival time are reached. This happens through Wald Chi-Squared Test ($\chi 2$) ,the calculated (Wald) values are compared with the tabular values at one degree of freedom for each variable and the level of significance is (0.05) as follows:

Table2 :Variables in the Equation

Step	Variables	B	SE	Wald	df	(Sig.)	Exp(B)
Step 1	Blood type	0.051	0.081	0.401	1	0.527	1.052
	Sex	0.016	0.106	0.022	1	0.882	1.016
	Marital status	0.173	0.085	4.115	1	0.042	1.188
	Region of Living	0.102	0.035	8.363	1	0.004	1.107
	The type of disease	0.193	0.063	9.404	1	0.002	1.213
	type of treatment	0.453	0.162	7.859	1	0.005	1.573
	Regularity in Receiving	1.127	0.109	106.600	1	0.000	3.085
	The age	-0.216-	0.101	4.599	1	0.032	0.805
Step 2	Blood type	0.051	0.081	0.400	1	0.527	1.052
	Marital status	0.174	0.085	4.185	1	0.041	1.190
	Living region	0.101	0.035	8.344	1	0.004	1.107
	The type of disease	0.194	0.063	9.461	1	0.002	1.214
	type of treatment	0.455	0.161	7.954	1	0.005	1.576
	receiving regularity	1.126	0.109	106.751	1	0.000	3.082
	The age	-0.217-	0.101	4.651	1	0.031	0.805
Step 3	Marital status	0.171	0.085	4.062	1	0.044	1.187
	Living region	0.102	0.035	8.399	1	0.004	1.107
	The type of disease	0.193	0.063	9.385	1	0.002	1.213
	Type of treatment	0.456	0.162	7.972	1	0.005	1.578
	Regularity in eceiving	1,122	0.109	106.402	1	0.000	3.072
	The age	-0.214-	0.101	4.516	1	0.034	0.807

From table 3 and by comparing the level of significance values (Sig) withe level of significance (0.05), it is noticed in the first step that the variables (marital status, area of residence, type of disease, and type of chemotherapy, regularity in receiving treatment, and age) are the significant variables and that the rest of the variables were non-significant and had no effect on the survival time.

The gender variable had the least effect and it has the lowest significant level of (0.882). Therefore it is deleted from the model in the second step. Moreover, in the second step, it also noted that the variables (marital status, area of residence, type of disease, type of chemotherapy, regularity in receiving treatment and age) are the significant variables except for the blood type variable that has no significant effect as it was less influential on the survival time. The level of significance was (0.527) and therefore it was removed from the model in the third step.

In the third step, it is noted that the survival of the variables (marital status, area of residence, type of disease, type of chemotherapy, regularity in receiving treatment, and age) are all significant variables affect the survival time, thus they remain in the model. The reduced model of the overall model will include the variables that maintained their significance in the last step which are (the marital status, the area of residence, the type of disease, and the type of chemotherapy , regularity in receiving treatment and age). Thus, the shortened form of the (cox) model is as follows:

- **Hazard Function**

$$h(t) = h\_0\ (t)\ \ exp\ (\ 0.171M.d + 0.102K.S + 0.193H.t + 0.456T.m + 1.122T.d - 0.214Yaş)$$

- **Survival Function**

$$S(t) = [S_0(t)]^{\exp(\ 0.171M.d+0.102K.S+0.193H.t+0.456T.m+1.122T.d-0.214Yaş)}$$

As for the values of the column (Exp(B)), they represent the estimated risk ratio. If its value is greater than one, it means that the risk is high and if it is less than one, it means that the risk is low. This value expresses the contribution of the independent variable to the risk when it increases more than he correct one in light of the rest of the other independent variables remaining constant.

For example, it is found that the value of (Exp(B)) for the disease type variable is equal to (1.213) which means that the risk rate increases by (21%) for each change in the disease type in light of the rest of the variables remaining constant. It was calculated [(1,213 - 1=-2,13*100=21,3)] are negative sign which means increased risk). To find out whether survival progression differs according to the type of disease, the reference cell coding method was used as the lowest level category which is acute lymphoblastic leukemia (ALL) is selected as a reference cell and compared against the rest of the other categories as follows:

Table 4. Hazard Ration Test for Disease Type Using Reference Cell

The type of disease	B	Wald	(Sig.)	Exp(B)
CLL	1.005	5.789	0.016	2.731
AML	-0.143	0.926	0.336	0.867
CML	0.402	7.367	0.007	1.495

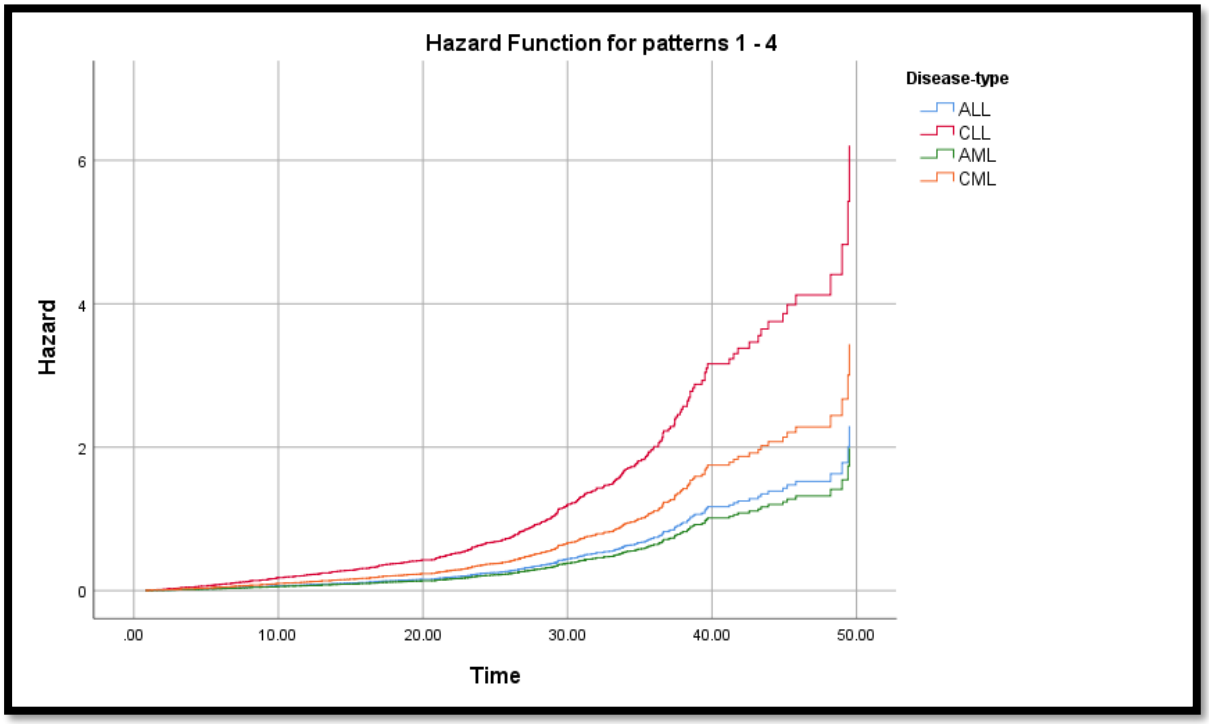

Figure 2. Hazard Ratio for Type of Disease Using the Reference Cell

From table (4) and Figure 2, it is found that the value of the Wald test for type (AML) was non-significant which means there are no significant differences between the risk rate of patients with type (AML) compared with patients with type (ALL. This is due to the level of significance for it was less than (0.05) and the value of the Wald test for patients with both types (CLL) and (CML) was significant.

Therefor, there are significant differences between the risk rate between patients with both types (CLL) and (CML) compared with infected patients with type (ALL). Referring to the Exp(B) value, it is noted that the estimated risk ratio for patients with type (AML) is (0.867) which means that the death rate is lower by (12.4%) for patients with type (AML) than for patients with type (ALL). Moreover, patients with type (CML) die at a rate of (49.5%) more than patients with type (ALL) and it is also noted that patients with type (CLL) die at a rate of (1.731%) times more than patients with type (ALL) .This explains the significance of the variable in the model. Thus, there are at least two of these types that have a risk ratio that differs significantly from the type (ALL).

- **Determine the Best Model:**

When testing the significance of the variables included in the model, several models nominated and the best model in predicting the risk function among all models can be determined through the Likelihood Ratio test which is distributed according to Chi- square distribution as follows:

Table 5: Likelihood Ratio Test Result to choose the Best Model

Step. No _	**-2 Log Likelihood**	***x*^2 Calculated**	**df**	**(Sig.)**
	-2 Log Likelihood = 4395.454			
Step 1	4256.558	138.896	8	0.000 4
Step 2	4256.580	138.874	7	0.000 1
Step 3	4256.972	138.481	6	0.000 0

According to table (5), it is noted that the first model that contains all the variables has a level of significance (0.0004) and that the calculated value was greater than the tabular value. Thus, it is less important than all other models .As well as for the second and third models, it is found that the level of significance for them was less than (0.05) . Consequently, it was found that the third model that contains variables (marital status, city of residence province, type of disease, treatment method used, regularity in treatment and age) is the most significant model among all other models where the level of significance was (0.0000).

- **Survival Times Analysis:**

Depending on the life table equations and dividing the survival times into equal periods of three months and by using the SPSS program, the following results were obtained.

Table 6. Life Table of Survival Data for Patients with Leukemia

Interval Start Time	Number Entering Interval	Number Withdrawing during Interval	Number Exposed to Risk	Number of Terminal Events	Proportion Terminating	Proportion Surviving	Cumulative Proportion Surviving at End of Interval	Hazard Rate
0	1168	31	1152.500	11	0.01	0.99	0.99	0.00
3	1126	63	1094.500	26	0.02	0.98	0.97	0.01
6	1037	78	998.000	26	0.03	0.97	0.94	0.01
9	933	56	905.000	22	0.02	0.98	0.92	0.01
12	855	49	830.500	23	0.03	0.97	0.89	0.01
15	783	31	767.500	26	0.03	0.97	0.86	0.01
18	726	67	692.500	21	0.03	0.97	0.84	0.01
21	638	99	588.500	39	0.07	0.93	0.78	0.02
24	500	88	456.000	33	0.07	0.93	0.72	0.03
27	379	75	341.500	43	0.13	0.87	0.63	0.04
30	261	41	240.500	25	0.10	0.90	0.57	0.04
33	195	55	167.500	29	0.17	0.83	0.47	0.06
36	111	32	95.000	25	0.26	0.74	0.35	0.10
39	54	10	49.000	8	0.16	0.84	0.29	0.06
42	36	7	32.500	5	0.15	0.85	0.24	0.06
45	24	11	18.500	2	0.11	0.89	0.22	0.04
48	11	7	7.500	4	0.53	0.47	0.10	0.00

The median survival time is 35.06

Table (6) consists of 9 columns, where each row is the period of stay and each period is divided into three months as the start time of the period starts from zero. It also includes the period up to the third month and the second period starts from the third month to less than six months and so on to 49 months. the second column represents the number of persons entering each period and shows the number of those still alive until the beginning of the current period .It is calculated as $n_{i_{-1}} = n_i - (c_i + D_i)$ where it is found that the number of persons entering at the beginning of the period is 1168 persons while those who remained less than six months in the second period n_2= 1168-(31+11)=1126 .

Their number was 1126 people and so on for the rest of the periods. The third column represents the number of people observed while the fourth column estimates the size of the actual sample which means how many cases were observed during the entry into the time period. For example the number of those entered at the beginning of the second month is calculated as (1126 - (63/2) = 1094.5) and an assumption is made with the case withdraws in the middle of the time period. The fifth column represents the number of whom the event (death) occurred in the time period. For example, at the beginning of the third month, it is found that whom the event (death) occurred were 26 people. The sixth column represents the

percentage of the dead while the seventh column is the percentage of the survivors. For example, there are 855 cases who entered the twelfth month.

The probability that the patient completed twelve months is (1-0.03 = 0.97). The eighth column represents the probability of survival at the end of each periodt_i, for example, the cumulative percentage of patients surviving until the end of the fifteenth month is (0.86) or (87%). The ninth and last column represents the risk function and is known as the probability of failure during a very small period of time. Assuming that the patient survives from the beginning of the period to its end, it was found that the greatest risk is at the time of survival in the thirty-sixth month when it reached (0.10). In addition, it was found that the median survival time is (35.06) months and that the probability of survival at this time is equal to (0.50). This is the time in which half of the cases under study are expected to survive or it is the time after which 50% of the individuals under the study are expected to survive.

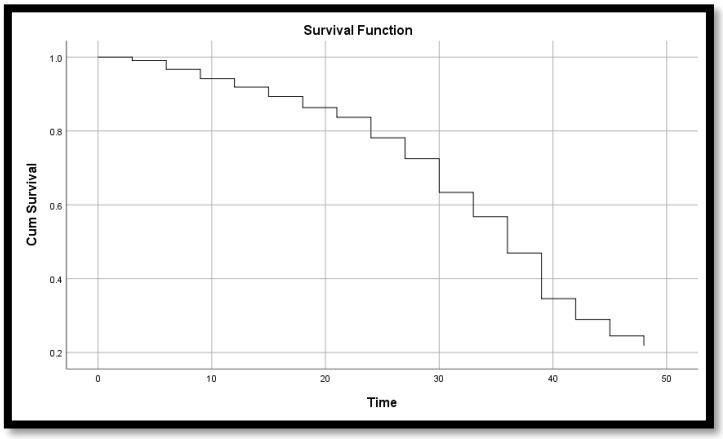

Figure 3. Curve of the Survival Function for Patients with Leukemia according to the Method of Life Tables.

Figure (3) shows the curve of the cumulative survival function in the life table and for all periods where each period is equal to three months. The vertical axis represents the cumulative survival function and the horizontal axis represents the time in months . It is noticed that the probability of survival times for infected patients is constantly decreasing until the probability of their survival (21) months which is (0.78) ,the probability that they will stay for a period of 24 months is (0.72) and the probability that they will stay for (45) months is (0.22).

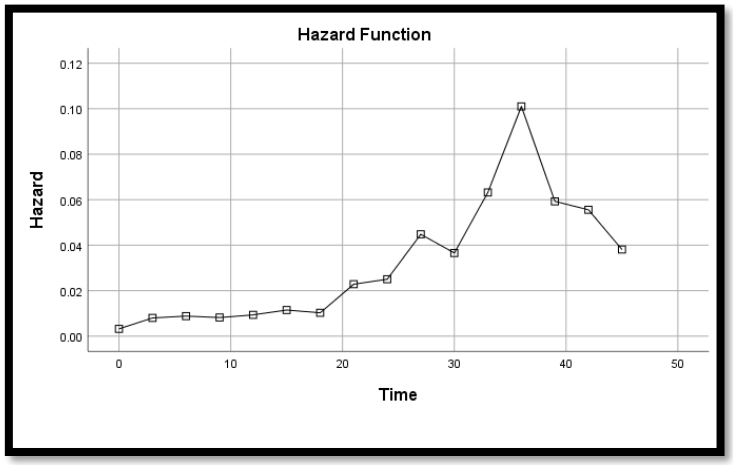

Figure 4. Curve of the Risk Function for Patients with Leukemia according to the Method of Life Tables.

Figure (4) represents the risk function for the life table and for all periods where each period is equal to three months. The vertical axis represents the risk function and the horizontal axis represents the time in months. It is noticed that the risk is low at the beginning of the period then begins to be increased at the twentieth month and then returns to be decreased in the thirtieth month as well as it returns to be raised until the thirty-sixth month then turns to be decreased in the thirty-ninth month. Furthermore, it is found that the highest risk rate is in the period (33-36) months as the risk rate in this period is (0.10) which is the largest rate among all other periods.

6. CONCLUSIONS

This study aimed at shedding light on the theoretical and practical importance of the (Cox) regression model in the analysis of survival, in addition it aimed at measuring the most important factors affecting the survival time of leukemia patients in the Republic of Yemen using the (Cox) model. Moreover, beside the above aims, this study aims at suggesting the best statistical model to determine the degree of risk facing patients with this disease, to estimate the survival and risk functions for this model and to form a Life Table.

All previous studies agreed on the importance of using the Cox regression model in survival analysis and these studies generally aimed at measuring the factors affecting survival time for a group of different phenomena some of which were applied in the medical field as in our study,some of which were applied in the economic field and others in the social field.

In each field, the variables of the study differed according to the study community and the time period spent in applying the study. This study concluded several results, the most important of which are the following:

- The (Cox) model does not depend on a specific distribution of survival times. Consequently, it can be used to indicate the effect of independent variables (risk factors) on the probability of survival as the model provides estimates for the coefficients of each variable. This allows evaluating the effect of multiple variables at the same time and showing their effect on survival time for people with leukemia.

- The results of the analysis have shown that the independent variables (risk factors) that maintained survival in the Cox model are: (age, marital status, type of disease, the province in which the patient lives, regularity in receiving treatment and type of chemotherapy) and it had a significant effect in the time of survival. However, the rest of the variables (sex and blood type) have not shown any significant effect on the time of survival. Furthermore, the model that contains the variables (age, marital status, type of disease, the governorate in which the patient lives, regularity in receiving treatment and chemotherapy type) is the best model among other models.

- The possibility of using the cox regression model in calculating both the survival and risk functions at any given time after estimating the survival and risk functions as well as the basic functions. Furthermore, the possibility of using life tables in analyzing the study data.

- Through the life table, it is noticed that the greatest risk in the survival time is the thirty-sixth month as it reached (0.10) which is greater than all other periods and that the median survival time was (35.06) months.

- There are differences in the incidence according to the type of disease in terms of the risk of death as acute lymphoblastic leukemia (ALL) is the most prevalent disease among all diseases with a rate of (65.8%) of the total patients. The proportions of patients with acute myeloid

leukemia (AML) and chronic myeloid leukemia (CML) were close to (16.8%) and (14.7) respectively. Moreover, the highest percentage of deaths was among patients with chronic myeloid leukemia (CML) which reached to (33.1%).

CONFLICT OF INTEREST

The authors stated that there are no conflicts of interest regarding the publication of this article.

AUTHORSHIP CONTRIBUTIONS

All authors contributed to the study conception and design. Material preparation, data collection and analysis were performed by Elias Al-samai and Sevil Senturk. All authors read and approved the final manuscript.

REFERENCES

[1] Tabachnick BG, Fidell LS, Ullman JB. Using Multivariate Statistics. Pearson Boston, MA; 2007.

[2] Liu ST. SAS, Survival Analysis Techniques for Medical Research; 2004.

[3] Walstra P, Wouters JTM, Geurts TJ. Survival analysis a practical approach. Dairy science & Technology, CRC Taylor & Francis Group. Published online 2005:267.

[4] Lee ET, Wang J. Statistical Methods for Survival Data Analysis. John Wiley & Sons; 2003.

[5] Alrun MB. Survival Analysis of the Registered Colorectal Cancer Cases in the Gaza Strip. BMC Public Health. Published online 2017.

[6] Marshall AW, Olkin I. Life Distributions. Springer; 2007.

[7] Okal M. Survival analysis of breast cancer patients in Gaza Strip. Published online 2010.

[8] Kamal SMM. Socio-economic determinants of age at first marriage of the ethnic tribal women in Bangladesh. Asian Population Studies, 2011;7(1):69-84.

[9] Burcu Küley Ağir. Survival and cox regression analyzes: A Case Study From Animals Science. Published Online 2017.

[10] Selim S, Sülükçüler S. Duration analysis of factors affecting smoking time: A Case Study of Türkiye. Bağımlılık Dergisi. 2023;24(4):475-486.

[11] Çilengiroğlu Öv. Evaluation of the first job finding periods of university graduates with cox regression model. Türkiye Sosyal Araştırmalar Dergisi. 2023;27(1):49-68.

[12] Klein JP, Moeschberger ML. Survival Analysis: Techniques for Censored and Truncated Data. Springer Science & Business Media; 2006.

[13] Kaplan EL, Meier P. Nonparametric estimation from incomplete observations. Journal of the American Statistical Association. 1958;53(282):457-481.

[14] Allison PD. Survival Analysis Using SAS: A Practical Guide. Second Edi. Sas Institute; 2010.

[15] Cox DR. Regression models and life-tables. Journal of the Royal Statistical Society: Series B (Methodological), 1972;34(2):187-202.

[16] O'Quigley J. Proportional Hazards Regression. Springer; 2008.

[17] Klein JP. Handbook of Survival Analysis; 2016.

[18] McCulloch WS, Pitts W. A logical calculus of the ideas immanent in nervous activity. The Bulletin Of Mathematical Biophysics. 1943;5(4):115-133.

[19] Walters SJ. What Is a Cox Model? Citeseer; 2009.

[20] Lawless JF. Statistical Models and Methods for Lifetime Data. John Wiley & Sons; 2011.

ESKİŞEHİR TECHNICAL UNIVERSITY JOURNAL OF SCIENCE AND TECHNOLOGY
A- APPLIED SCIENCES AND ENGINEERING

2023, 24(3), pp. 207-215, DOI:10.18038/estubtda.1335496

RESEARCH ARTICLE

FABRICATION OF A NOVEL FeB-B_4C COMPOSITE POWDER AND EVALUATING ITS POTENTIAL FOR ENERGY STORAGE APPLICATIONS

Suna AVCIOĞLU

Department of Metallurgical and Materials Engineering, Faculty of Chemistry and Metallurgy, Yıldız Technical University, Istanbul, Turkey

ABSTRACT

The development of energy storage devices is critical for humanity to declare its independence from fossil fuels. Supercapacitors and batteries are rapidly growing technologies. Nevertheless, their current progress is still insufficient to meet global demand. Therefore, advances in new generation and tailored materials for energy storage applications are urgently needed. Herein, for the first time, a novel composite of FeB-B_4C powder was synthesized by a one-pot sol-gel technique, and its potential as an active material for electrodes in energy storage devices was investigated. The phase analysis showed that a composite powder containing 91±5% B_4C and 9±5% FeB was obtained without unwanted excess phases such as graphite, boron, or iron oxide. Scanning electron microscopy images of the composite powder revealed the formation of elongated boron carbide particles connected with spherical iron boride ones. The size of the boron carbide particles was found to be in the range of 1 to 10 µm, while the iron boride particles were formed in the submicron range. The synthesized composite's electrochemical properties were investigated using a three-electrode set-up. Cyclic voltammetry (CV) and galvanostatic charge/discharge tests (GCD) were employed. The results obtained indicate the pseudocapacitive behavior of the electrodes with a specific capacitance of 8.28 F/g.

Keywords: Iron boride, Boron carbide, Composite, Energy storage, Supercapacitor

1. INTRODUCTION

Pollution and global warming are some of the problems associated with modern society's dependence on fossil fuels due to energy shortages and rising fuel costs [1]. As well as the production of renewable energy, the storage of produced energy is one of the obstacles to reducing dependence on fossil fuels [2]. With the rapid development of the industry, the demand for high-capacity energy storage devices powered by green energy has become increasingly crucial. In terms of environmental impact and resource sustainability, supercapacitors are expected to have a great impact on the transition to greener energy consumption [3].

In recent research progress, the pseudocapacitive or battery type materials (metal sulfides, metal nitrides and metal carbides) have been effectively studied for supercapacitor electrodes due to the existence of their unique redox mechanism [4]. Many transition metal carbides such as, SiC, TiC, V_4C_3, WC, MoC and B_4C have attracted attention for energy storage applications [5]. SiC nanocauliflowers (NCs) were investigated by Amit Sanger et al. as an electrode material for supercapacitors, which increased the high specific capacitance of SiC NCs up to about 300 F/g and produced symmetric devices that delivered high energy (31.43 Wh/kg) and power density (18.8 kW/kg) with good cyclic stability (94%) at 1 M Na_2SO_4 [4]. Two-dimensional vanadium carbide as super capacitor electrode material with aqueous electrolyte was studied by Qingmin shan et al., which achieved the excellent specific capacitance of 487 F/g [5]. Joseph Halim et al., demonstrated the large-scale synthesis and delamination of 2D Mo_2CT electrodes in supercapacitors, capacitances as high as 700 F cm^{-3} and high-capacity retention

*Corresponding Author: suna.avcioglu@yildiz.edu.tr
Received:01.09.2023 Published:22.09.2023

about 10,000 cycles. Besides Mo_2CTx tested the electrode material for Li-ions achieved the reversible capacities of 250 mAh/g [6].

Among the carbide materials, boron carbide (B_4C) is a semiconductor with high chemical resistance [7]. Besides, it has many unique properties that can be useful for energy storage devices, such as high thermal stability, high melting point, low density, and low thermal expansion coefficient [8]. For these reasons, boron carbide (B_4C) has been used in a number of electrochemical energy storage systems, including zinc-air, vanadium redox flow, lithium-oxygen, and lithium-sulfur batteries [9–12]. Wen-Bin Luo et al. could synthesize B_4C nanowires from carbon nanotubes, and they utilized B_4C nanowires as a novel bifunctional electrocatalyst in battery applications [13]. They also reported that B_4C nanowire-based electrodes could be operated up to 2.2 V voltage even after 120 cycles. B_4C nanowires grown in situ on carbon nanofibers (B_4C@CNF) were used by Liu Luo et al. to fabricate a novel cathode substrate, which also achieved 9 mAh/cm^2 areal capacity and excellent capacity retention of 80% after 500 cycles [14]. In addition, Chang et al. showed that the core-shell structure B_4C@C could potentially be an electrode material for all solid-state micro-supercapacitors [15]. In our recent study, we demonstrate that the morphological differences of boron carbide particles influence the electrochemical performance of supercapacitor electrodes made of these particles [16]. So, as indicated in previous studies boron carbide has a great potential for use in energy storage devices. Nevertheless, boron carbide lacks electrical conductivity, and its' slower ionic transport kinetics need to be enhanced to improve its electrochemical performance.

Recently, metal borides have been proposed as co-catalyst for photocatalysis and electrocatalysis because of their charge-transfer enhancement [17–19]. Moreover, the electrochemical properties of some of the metal borides such as TiB, VB, and CoB have been tested for energy storage applications [20,21]. In this study, for the first time in the literature, FeB-B_4C composite powder was synthesized, and its electrochemical properties were investigated. The phase content and morphological features of the composite powder, as well as the charge storage mechanism and performance of the electrodes were revealed and discussed.

2. EXPERIMENTAL

2.1. Synthesis and Characterization of Composite Particles

For the synthesis of iron boride-boron carbide composite particles, analytical grade starting chemicals were purchased from Merck and used without additional purification. All solid starting materials were directly added to glycerin according to the molar ratio given in Table 1. Using a hot plate, the mixture was vigorously magnetic stirred in an oil bath to ensure homogeneous heat distribution. The temperature of the mixture was then gradually increased over an hour to 150°C, where it remained for another hour under vigorous magnetic stirring (450 rpm). After this process, the formed gel was poured into alumina crucibles and cooled to room temperature. Then the gel was calcinated at 675 °C for 2 hours using a muffle furnace to burn off extra carbon. Finally, the calcined product was subjected to a final heat treatment at 1500 °C for 5 hours in a tube furnace under argon (500 ml/min) to obtain composite particles.

Table 1. Molar ratios of starting chemicals.

Glycerin ($C_3H_8O_3$)	**Tartaric Acid ($C_4H_6O_6$)**	**Boric Acid (H_3BO_3)**	**Iron (III) Nitrate ($Fe(NO_3)_3.9H_2O$)**
1 mol	0.25 mol	1 mol	0.25 mol

The phases present in the synthesized powder were analyzed by X-ray diffraction technique (XRD, Bruker D2 Phaser) using Cu Kα radiation (λ = 1.540 Å, 30 kV, and 10 mA) in the range of 10° to 80° with a scanning speed of 0.5°/min. Scanning electron microscopy (SEM, Zeiss EVO LS 10) was used

to examine the particle morphology. Elemental point analysis (EDS-Thermo scientific energy dispersive X-ray detector) was performed to examine the elemental distribution.

2.2. Fabrication of Electrodes and Electrochemical Measurements

To fabricate a working electrode, firstly, a fine paste was prepared by mixing 0.085g of as-synthesized powder, 0.01g C65 conductive carbon black, and 0,005 g poly (vinylidene fluoride) binder with 0.025 mL of NMP (N,N-dimethyl pyrrolidinone) solution. The mixture was placed in a 15 mL glass bottle with a closed lid, and to obtain a homogeneous mixture magnetic stirring was applied at room temperature for 24 hours. The obtained fine mixture was poured onto a nickel foam substrate (1 × 1 cm^2). The coated substrate was then allowed to dry for 24 hours at 80 °C before being employed as a working electrode in all electrochemical experiments. The substrate was coated with 10 mg of active material.

A potentiostat/galvanostat (Metrohm-Vionic) electrochemical workstation was used to examine the electrochemical characteristics of the electrode at room temperature (~25 °C). A three-electrode setup with an aqueous 6 M KOH solution as the electrolyte was used for all electrochemical tests. In the assembled cell, the fabricated electrode containing synthesized particles acts as the working electrode, a Pt spring as the counter electrode, and Ag/AgCl as the reference electrode. Cyclic voltammetry (CV) was performed for different scan rates of 5, 10, 25, 50, 75, and 100 mVs-1. Galvanostatic charge/discharge testing was performed at different charge/discharge current densities (0.5, 1, and 2 Ag-1) in the constant potential window from 0 to 0.4 V.

3. RESULTS AND DISCUSSION

The phase pattern of as-synthesized powders provided by XRD analysis is shown in Figure 1. The pattern indicates that synthesized powder does not contain any amorphous phase, like amorphous carbon. Phase determination carried out by using HighScore Software shows that the powder contains two crystalline phases. The main phase was found to be boron carbide (CoD: 96-223-5963) with a 91±5% ratio. The observed secondary phase was indexed as iron boride (CoD: 96-101-0478) with a 9±5% ratio. Besides these two crystalline phases, no other residual oxide phase, such as boron oxide or iron oxide, was not observed.

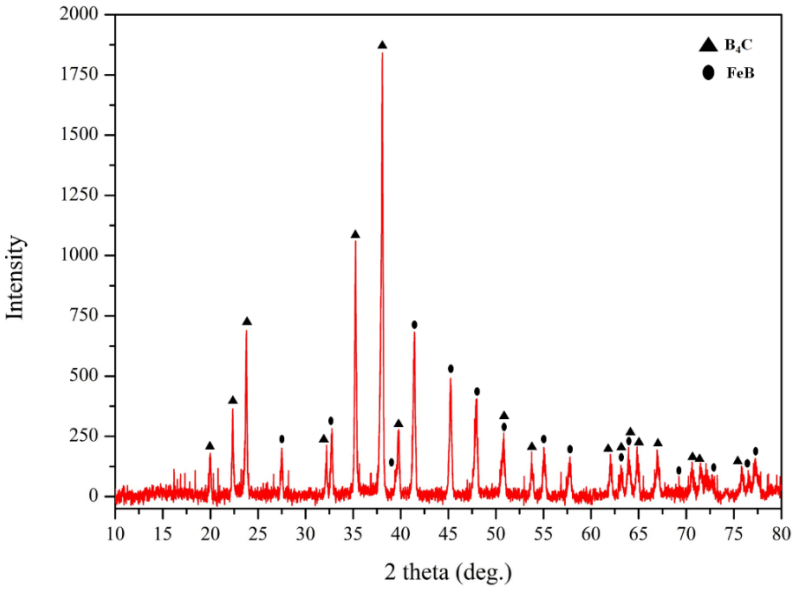

Figure 1. The XRD pattern of as-synthesized powder.

The secondary electron SEM image of the synthesized powder is presented in Figure 2-a. The image shows that most of the particles have elongated complex-shaped morphology. Besides, the surface texture of the particles is observable from the secondary electron SEM image (Figure 2-a). Straight-line marks on the surface of the particles were detected and highlighted with red arrows in Figure 2-a. The line-shaped marks originated because of non-completed stacked crystalline layers of boron carbide, and the marks indicate that the particles were grown via the lateral growth mechanism. The lateral growth of the particles generally results in the formation of particles with a high aspect ratio. Thus, the observed elongated complex-shaped morphology should be related to the dominant growth mechanism in the formation of particles during the final heat treatment stage. The approximate size of the particles was measured from SEM images using Image-J software. It is seen that the size of elongated complex-shaped particles is in the range of 1 to 10 µm. Furthermore, in addition to the micron-sized particles, sub-micron-sized particles with spherical morphology were observed, and these particles were emphasized with red circles in Figure 2-a. Moreover, spherical particles are generally seen as consolidated on the tip of the elongated ones. To reveal the chemical differences between these two types of particles, a backscattered SEM image was obtained and EDX analysis was carried out (Figures 2-b to d). The backscattered SEM image reveals that sub-micron-sized spherical particles appear brighter than elongated complex-shaped ones. This observation is evident that the iron boride phase forms the sub-micron-sized spherical particles. EDX analysis results are presented in Figures 2-c and d, also confirming that the sub-micron-sized spherical particles contain a high amount of iron (EDX-point 1). On the contrary, no iron was detected on EDX-point 2. Moreover, it's known that metal additives promote the uniaxial growth of carbides and nitrides [22,23]. So, it can be concluded that during the final heat treatment, iron boride enhances the lateral growth of boron carbide and particles formed in elongated complex-shaped morphology, unlike boron carbide particles' well-known polyhedral equiaxed morphology [24–26].

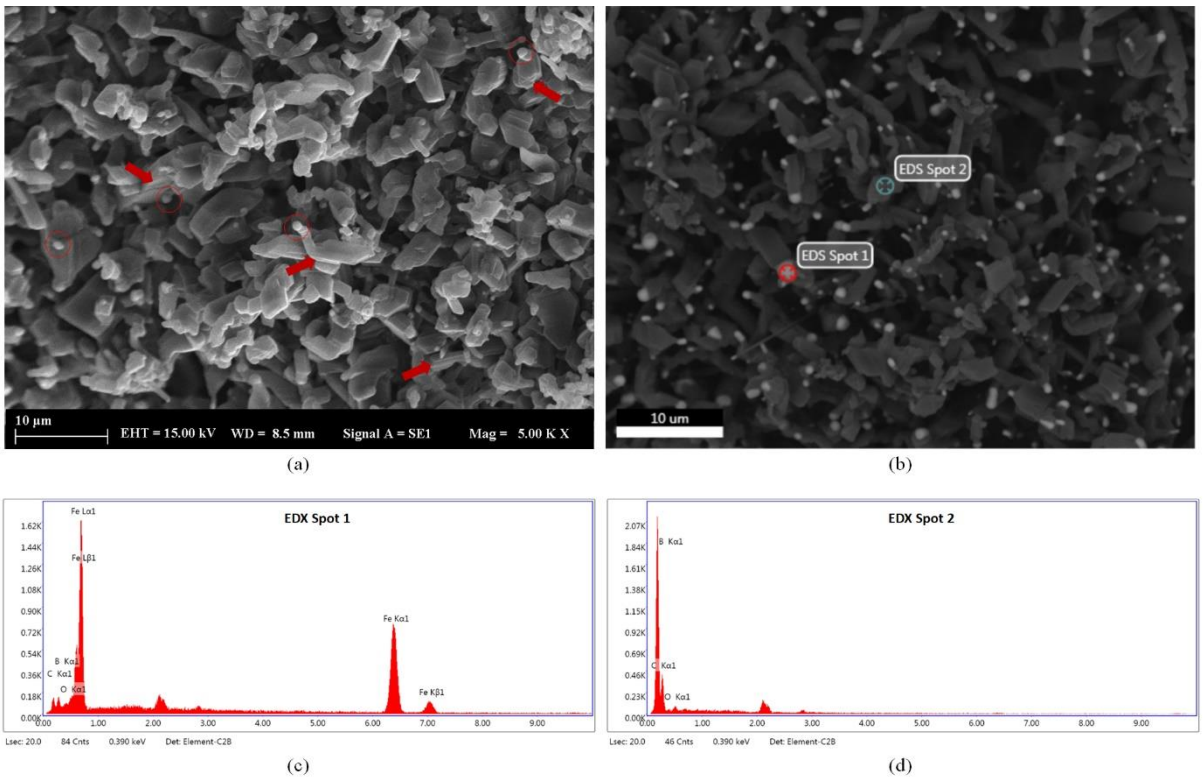

Figure 2. The scanning electron microscopy images and elemental point analysis results of synthesized powder. (a) secondary electron image, (b) backscattered electron image and EDS points, (c) elemental composition of point 1, and (d) elemental composition of point 2.

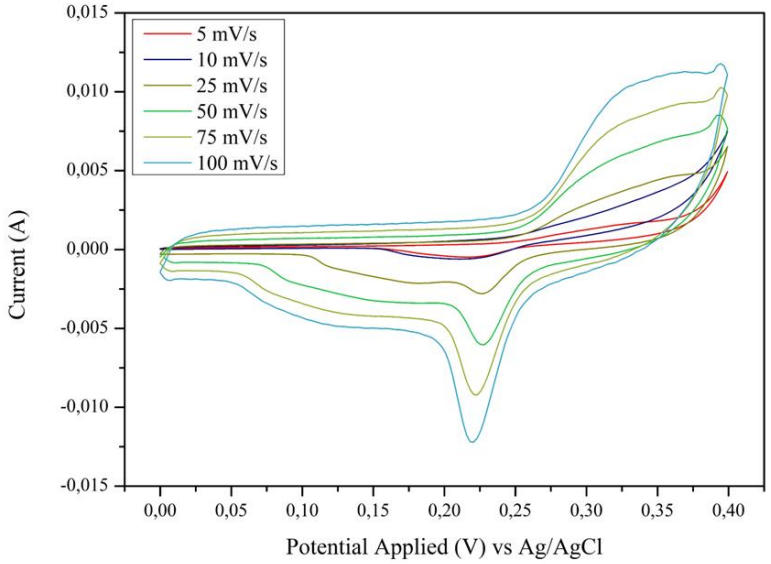

Figure 3. Cyclic voltammetry (CV) curves of the FeB-B_4C electrode at different scan rates in the range of 5 to 100 mV/s.

In order to evaluate the storage mechanism of the synthesized powder-based FeB-B_4C composite electrode, cyclic voltammetry (CV) analysis was performed. Figure 3 shows the cyclic voltammograms of the electrode recorded at different scan rates between 5 and 100 mV/s over a potential working window of 0-0.4 V in an aqueous solution of 6 M KOH. The obtained CV curves exhibit an identical profile, showing the film's strong reversibility in the 6 M KOH electrolyte. It is seen that the area under CV curves increases with the scan rate. This phenomenon can be explained by limited diffusion at high scan rates, so higher current occurs, and higher current results in an increase in CV curve area [27]. Moreover, clear oxidation and reduction peaks were determined in the CV curves, demonstrating the electrode's pseudocapacitive behavior. In addition, a slight shift in the potential positions of both the oxidation and reduction peaks was observed with increasing scan rate. This observation may correspond to the electrodes' low polarization [28].

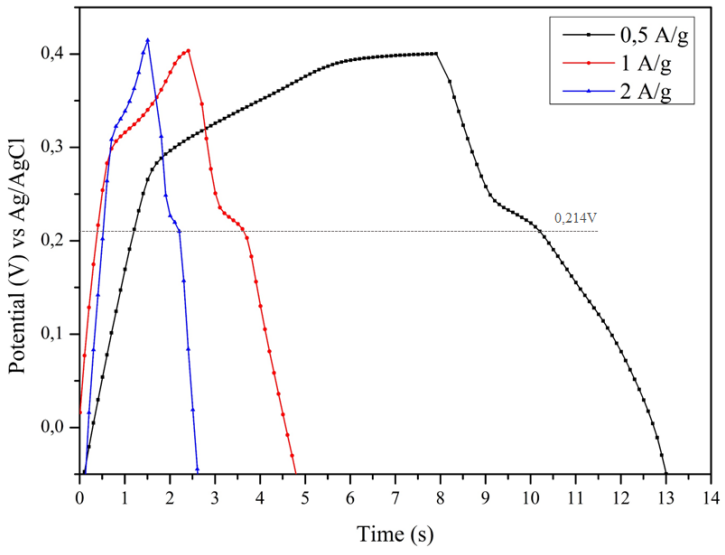

Figure 4. Galvanostatic charge-discharge (GCD) curves of the FeB-B_4C electrode at current densities of 0.5 A/g, 1 A/g, and 2 A/g.

To assess the performance of the electrode materials for energy storage devices, galvanostatic charge-discharge (GCD) was employed. The GCD profiles obtained at various scan rates are displayed in Figure 5 for comparison. It can be seen that the discharge curves are not linear and exhibit a potential slope just above 0.214 V, suggesting the presence of pseudo-capacitance behavior, which is consistent with the CV measurements. Equation 1 is used to calculate the specific capacitance of electrode materials from galvanostatic discharge curves.

$$C_s = \frac{\Delta T \times i}{\Delta V \times m} \tag{1}$$

$\boldsymbol{i}$: current (A), $\Delta \boldsymbol{T}$: the discharge time (s), $\Delta \boldsymbol{V}$: potential window (V), $\boldsymbol{m}$: mass of active material (g)

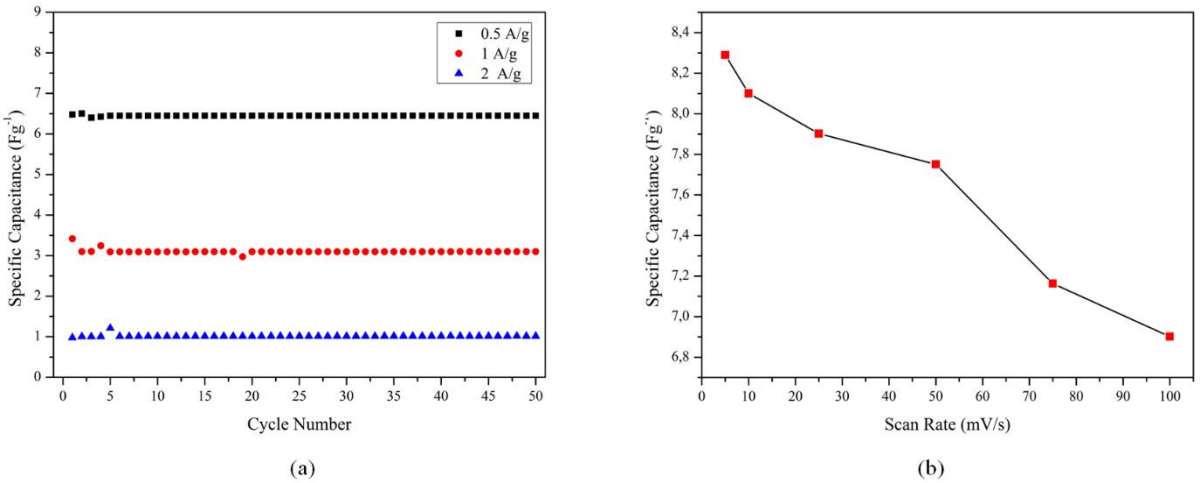

Figure 5. Comparative specific capacitance values of the FeB-B_4C electrode. (a) specific capacitance values calculated from GCD curves in a function of cycle number and current densities, (b) specific capacitance values calculated from CV curves in a function of scan rate.

The specific capacitance values obtained from the GCD curves for different scan rates and during 50 cycles are shown in Figure 5-a. It can be seen that the specific capacitance values are constant up to 50 cycles, indicating the stability of the electrodes. Moreover, the calculated specific capacitance value at 0.5 A/g is 6.5 F/g, decreasing to 1 F/g with increasing current density to 2 A/g. The decrease in specific capacitance at high current density is likely caused by the electrolyte ions' adverse accessibility to the electrode's core active sites [29]. Determination of the specific capacitance values from GCD curves is a good approach to characterize the electrodes' stability through long cycles. However, since the potential does not change linearly with time during discharge, equation 1 can only provide an approximate specific capacitance value. Another way to estimate the more accurate specific capacitance value for pseudo-capacitive electrodes is to calculate from CV curves. Equation 2 was utilized to calculate the specific capacitance values from the CV curves**,** and the results are presented in Figure 5-b.

$$C_s = \frac{\int_{V1}^{V2} I(V)dV}{mv(V2 - V1)} \tag{2}$$

$\int_{V1}^{V2} \boldsymbol{I}(\boldsymbol{V})\boldsymbol{dV}$: area under CV curve, $\boldsymbol{m}$: mass of active material (g), $\boldsymbol{v}$: scan rate (V/s)

It is seen from Figure 5-b that the highest specific capacitance value of 8.28 F/g was obtained at 5 mV/s, and as expected, it gradually decreases with increasing scan rate. The lowest specific capacitance value calculated from the CV curves was found to be 6.9 F/g, which is slightly higher than the specific capacitance calculated from the GCD discharge curve.

In summary, it can be noted from the electrochemical analysis results that synthesized FeB-B_4C composite powders have the potential to be a candidate for supercapacitor applications with a pseudocapacitive charge storage behavior. The capacitive performance can be further increased by decreasing particle size, increasing specific surface area, improving the FeB:B_4C phase ratio, and optimizing the cell conditions such as electrolyte type and molarity.

4. CONCLUSION

In this study, FeB-B_4C composite powder without any residual phases, such as graphite, boron oxide, or iron oxide, was synthesized by one-pot sol-gel technique at 1500°C. The morphological inspections showed that a composite of elongated boron carbide particles and sub-micron sized spherical FeB particles formed. The electrochemical properties of the synthesized composite powder investigated by three-electrode set-up. The pseudo-capacitive behavior of electrodes was revealed from the observed oxidation/reduction peaks and potential oblique in the cyclic voltammogram and discharge profiles of electrodes, respectively. The highest specific capacitance value of 8.28 F/g was calculated from the CV curves at a scan rate of 5 mV/s. The synthesized FeB-B_4C composite powder can be used as an active material for fabricating positive electrodes for supercapacitors. The performance of electrodes can be improved by optimizing the particle size and phase ratio.

ACKNOWLEDGEMENTS

The author is grateful for the financial support from The Scientific and Technological Research Council of Turkey (TUBITAK) and Yıldız Technical University under contract numbers of 120M651 and FBA-2023-5301, respectively.

CONFLICT OF INTEREST

The author stated that there are no conflicts of interest regarding the publication of this article.

REFERENCES

[1] Zandalinas SI, Fritschi FB, Mittler R. Global Warming, Climate Change, and Environmental Pollution: Recipe for a Multifactorial Stress Combination Disaster. Trends in Plant Science 2021;26(6):588–99.

[2] Simons S, Schmitt J, Tom B, Bao H, Pettinato B, Pechulis M. Chapter 10 - Advanced concepts. In: Brun K, Allison T, Dennis R (editors). Thermal, mechanical, and hybrid chemical energy storage systems. London: Academic Press, an imprint of Elsevier; 2021. p. 569–96.

[3] Olabi AG, Abbas Q, Al Makky A, Abdelkareem MA. Supercapacitors as next generation energy storage devices: Properties and applications. Energy 2022;248:123617.

[4] Sanger A, Kumar A, Kumar A, Jain PK, Mishra YK, Chandra R. Silicon Carbide Nanocauliflowers for Symmetric Supercapacitor Devices. Ind. Eng. Chem. Res. 2016;55(35):9452–8.

[5] Liu W, Soneda Y, Kodama M, Yamashita J, Hatori H. Low-temperature preparation and electrochemical capacitance of WC/carbon composites with high specific surface area. Carbon 2007;45(14):2759–67.

[6] Halim J, Kota S, Lukatskaya MR, Naguib M, Zhao M-Q, Moon EJ, Pitock J, Nanda J, May SJ, Gogotsi Y, Barsoum MW. Synthesis and Characterization of 2D Molybdenum Carbide (MXene). Adv. Funct. Mater. 2016;26(18):3118–27.

[7] Shiota I, Miyamoto Y (editors). Functionally grated materials 1996. Amsterdam: Elsevier; 1997.

[8] Avcıoğlu S, Kaya F, Kaya C. Morphological evolution of boron carbide particles: Sol-gel synthesis of nano/micro B4C fibers. Ceramics International 2021;47(19):26651–67.

[9] Song S, Yu L, Ruan Y, Sun J, Chen B, Xu W, Zhang J-G. Highly efficient Ru/B4C multifunctional oxygen electrode for rechargeable Li O2 batteries. Journal of Power Sources 2019;413:11–9.

[10] Song S, Xu W, Zheng J, Luo L, Engelhard MH, Bowden ME, Liu B, Wang C-M, Zhang J-G. Complete Decomposition of Li2CO3 in Li-O2 Batteries Using Ir/B4C as Noncarbon-Based Oxygen Electrode. Nano Lett 2017;17(3):1417–24.

[11] Song N, Gao Z, Zhang Y, Li X. B4C nanoskeleton enabled, flexible lithium-sulfur batteries. Nano Energy 2019;58:30–9.

[12] Wang H, Ma C, Yang X, Han T, Tao Z, Song Y, Liu Z, Guo Q, Liu L. Fabrication of boron-doped carbon fibers by the decomposition of B4C and its excellent rate performance as an anode material for lithium-ion batteries. Solid State Sciences 2015;41:36–42.

[13] Luo W-B, Chou S-L, Wang J-Z, Liu H-K. A B 4 C nanowire and carbon nanotube composite as a novel bifunctional electrocatalyst for high energy lithium oxygen batteries. J. Mater. Chem. A 2015;3(36):18395–9.

[14] Luo L, Chung S-H, Yaghoobnejad Asl H, Manthiram A. Long-Life Lithium-Sulfur Batteries with a Bifunctional Cathode Substrate Configured with Boron Carbide Nanowires. Adv Mater 2018;30(39):e1804149.

[15] Chang Y, Sun X, Ma M, Mu C, Li P, Li L, Li M, Nie A, Xiang J, Zhao Z, He J, Wen F, Liu Z, Tian Y. Application of hard ceramic materials B4C in energy storage: Design B4C@C core-shell nanoparticles as electrodes for flexible all-solid-state micro-supercapacitors with ultrahigh cyclability. Nano Energy 2020;75:104947.

[16] Avcıoğlu S, Buldu-Akturk M, Erdem E, Kaya F, Kaya C. Boron Carbide as an Electrode Material: Tailoring Particle Morphology to Control Capacitive Behaviour. Materials (Basel) 2023;16(2).

[17] Avcıoğlu C, Avcıoğlu S, Bekheet MF, Gurlo A. Photocatalytic Overall Water Splitting by SrTiO 3 Progress Report and Design Strategies. ACS Appl. Energy Mater. 2023;6(3):1134–54.

[18] Avcıoğlu C, Avcıoğlu S, Bekheet MF, Gurlo A. Solar hydrogen generation using niobium-based photocatalysts: design strategies, progress, and challenges. Materials Today Energy 2022;24:100936.

[19] Wang D, Song Y, Zhang H, Yan X, Guo J. Recent advances in transition metal borides for electrocatalytic oxygen evolution reaction. Journal of Electroanalytical Chemistry 2020;861:113953.

[20] Yang HX, Wang YD, Ai XP, Cha CS. Metal Borides: Competitive High Capacity Anode Materials for Aqueous Primary Batteries. Electrochem. Solid-State Lett. 2004;7(7):A212.

[21] Zhang L, Chai S-S, Zhang W-B, Guo S-B, Han X-W, Guo Y-W, Bao X, Ma X-J. Cobalt boride on clay minerals for electrochemical capacitance. Applied Clay Science 2022;218:106416.

[22] Li J, Lin H, Chen Y, Su Q, Huang Q. The effect of iron oxide on the formation of boron nitride nanotubes. Chemical Engineering Journal 2011;174(2-3):687–92.

[23] Kriegesmann J. 2.04 - Processing of Silicon Carbide-Based Ceramics. In: Sarin VK, Mari D, Llanes L, Nebel CE (editors). Comprehensive hard materials. Amsterdam, Waltham: Elsevier; 2014. p. 89–175.

[24] Avcıoğlu S, Buldu M, Kaya F, Kaya C. Chapter 20 - Synthesis of nuclear-grade nano-sized boron carbide powders and its application in LDPE matrix composites for neutron shielding. In: Low I-M, Dong Y (editors). Composite materials: Manufacturing, properties, and applications. Amsterdam, Netherlands: Cambridge, MA; Elsevier; 2021. p. 543–79.

[25] Avcıoğlu S, Buldu M, Kaya F, Üstündağ CB, Kam E, Menceloğlu YZ, Kaptan HY, Kaya C. Processing and properties of boron carbide (B4C) reinforced LDPE composites for radiation shielding. Ceramics International 2020;46(1):343–52.

[26] Avcioglu S, Kaya F, Kaya C. Effect of elemental nano boron on the transformation and morphology of boron carbide (B4C) powders synthesized from polymeric precursors. Ceramics International 2020;46(11):17938–50.

[27] Ramachandran R, Xuan W, Zhao C, Leng X, Sun D, Luo D, Wang F. Enhanced electrochemical properties of cerium metal-organic framework based composite electrodes for high-performance supercapacitor application. RSC Adv 2018;8(7):3462–9.

[28] Hadji F, Omari M, Mebarki M, Gabouze N, Layadi A. Zinc doping effect on the structural and electrochemical properties of LaCoO3 perovskite as a material for hybrid supercapacitor electrodes. Journal of Alloys and Compounds 2023;942:169047.

[29] Yavuz A, Ozdemir N, Erdogan PY, Zengin H, Zengin G, Bedir M. Nickel-based materials electrodeposited from a deep eutectic solvent on steel for energy storage devices. Appl. Phys. A 2019;125(8):1–10.